Star Cluster Formation and Feedback

M. R. Krumholz, M. R. Bate, H. G. Arce, J. E. Dale, R. Gutermuth, R. I. Klein, Z. Y. Li, F. Nakamura, Q. Zhang

August 13, 2014

Disclaimer

Star Cluster Formation and Feedback

Mark R. Krumholz
University of California, Santa Cruz

Matthew R. Bate
University of Exeter

Héctor G. Arce
Yale University

James E. Dale
Excellence Cluster "Universe" and Ludwig-Maximillians-University

Robert Gutermuth
University of Massachusetts, Amherst

Richard I. Klein
University of California, Berkeley and Lawrence Livermore National Laboratory

Zhi-Yun Li
University of Virginia

Fumitaka Nakamura
National Astronomical Observatory of Japan

Qizhou Zhang
Harvard-Smithsonian Center for Astrophysics

Stars do not generally form in isolation. Instead, they form in clusters, and in these clustered environments, newborn stars can have profound effects on one another and on their parent gas clouds. Feedback from clustered stars is almost certainly responsible for a number of otherwise puzzling facts about star formation: (1) it is an inefficient process that proceeds slowly when averaged over galactic scales; (2) most stars disperse from their birth sites and dissolve into the galactic field over timescales ≪1 G.y.; and (3) newborn stars follow an initial mass function (IMF) with a distinct peak in the range 0.1–1 $M_\odot$, rather than an IMF dominated by brown dwarfs. In this review, we summarize current observational constraints and theoretical models for the complex interplay between clustered star formation and feedback.

1. INTRODUCTION

1.1. Why is Feedback Essential?

Newborn stars have profound effects on their birth environments, and any complete theory for star formation must include them. Perhaps the best argument for this statement is an image such as Fig. 1, which shows 30 Doradus, the largest HII region in the Local Group, powered by the cluster NGC 2070 and its 2400 OB stars (*Parker,* 1993). The figure illustrates several of the routes by which young stars can influence their surroundings. The red color shows 8-μm emission, marking where gas has been warmed by far ultraviolet (UV) radiation from young stars. The green color traces Hα, indicating where ionizing radiation has converted the ISM to a warm ionized phase. Finally, blue shows X-ray emission from an ~10^7-K phase created by shocks in the fast winds launched by the O stars. The entire region is expanding at ~25 km s^{-1} (*Chu and Kennicutt,* 1994). Any theory for how NGC 2070 arrived at its present state must address the role played by these processes, and several others such as protostellar outflow feedback and radiative heating by infrared (IR) light. These are not visually apparent in Fig. 1, but can be seen clearly in other regions, and are perhaps equally important.

In addition to the visual impression provided by Fig. 1 and similar observations, there are a number of more subtle but equally compelling arguments for the importance of
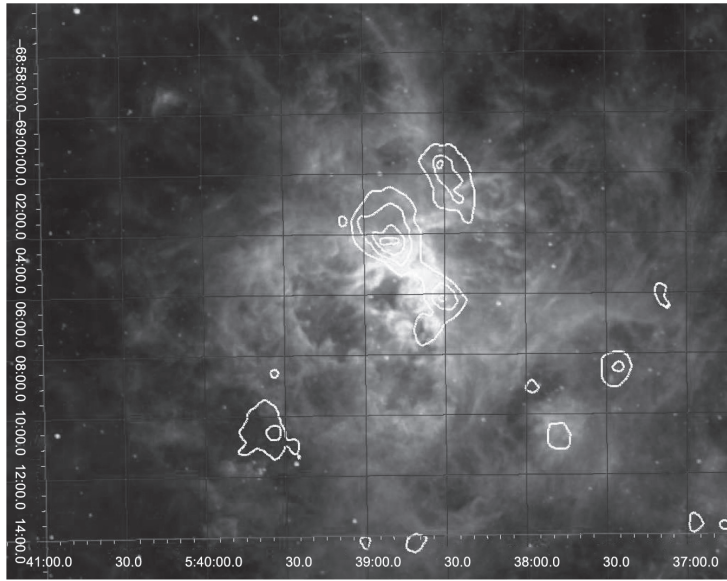
Fig. 1. Image of 30 Doradus: 8 μm, Hα, and 0.5–8 keV X-rays. White contours show ^{12}CO(1–0) emission. Figure taken from *Lopez et al.* (2011).

stellar feedback for cluster formation. The first, which dates back to the seminal work of *Zuckerman and Evans* (1974), is based on comparing the molecular mass M_{gas} to the star-formation rate $\dot{M}_*$ — either in an entire galaxy, or in a smaller region defined by a specified volume or column density threshold — to deduce a characteristic depletion time $t_{dep} = M_{gas} = \dot{M}_*$. Note that this should not be confused with the timescale over which star formation in a particular cloud takes place, as diagnosed, for example, by the stellar age spread (see the chapter by Soderblom et al. in this volume). The two are identical only if star formation proceeds until all the gas is converted to stars, and in general, the depletion time is 1–2 orders of magnitude larger.

While Zuckerman and Evans applied this technique to the low-density molecular gas traced by low-J CO emission, and numerous modern studies have done the same (see the chapters by Dobbs et al. and Padoan et al. in this volume), it has also become possible in the last 10 years to perform the same analysis for tracers of the denser regions from which clusters presumably form. Techniques for studying such regions include the low-J lines of heavy rotor molecules such as HCN, HCO$^+$, and CS (which have critical densities $\geq 10^4$ cm^{-3}), thermal emission from cold dust at submillimeter wavelengths, and dust extinction at near-IR wavelengths. The consensus from such studies is that the depletion time is always ~1–3 orders of magnitude longer than the free-fall time $t_{ff} \sim 1/\sqrt{G\rho}$, where ρ is the characteristic density selected by the tracer (*Krumholz and Tan,* 2007; *Evans et al.,* 2009; *Juneau et al.,* 2009; *Krumholz et al.,* 2012a; *Federrath,* 2013). In contrast, numerical simulations of star cluster formation that do not include any form of feedback generally produce $t_{dep} \sim t_{ff}$ (e.g., *Klessen and Burkert,* 2000, 2001; *Bate et al.,* 2003; *Bonnell et al.,* 2003).

Magnetic fields alone are unlikely to prevent this outcome. Observations suggest that the median cloud is magnetically supercritical by a factor of 2 (*Crutcher,* 2012, and references therein), and simulations indicate that a magnetic field of this strength only decreases the star-formation rate by a factor of a few compared to the purely hydrodynamic case (*Price and Bate,* 2009; *Padoan and Nordlund,* 2011; *Federrath and Klessen,* 2012) (see also the chapter by Padoan et al. in this volume). Reduction of the star-formation rate by feedback, perhaps in conjunction with magnetic fields, is a prime candidate to resolve this problem.

A second, closely related argument has to do with the fraction of stars found in bound clusters. Most regions of active star formation are much denser than the field (e.g., *Gutermuth et al.,* 2009). We will refer to these regions as clusters, defined roughly as suggested by *Lada and Lada* (2003): a collection of physically-related stars within which the stellar mass density is $\gg 1$ M$_\odot$ pc^{-3} [compared to ~0.01 in the field near the Sun (*Holmberg and Flynn,* 2000)], and where the total number of stars is greater than several tens. Such regions are typically ~1–10 pc in size, and, at least when they are young, also contain gas with a mass density greatly exceeding that of the stars. We do not require, as do some authors interested primarily in N-body dynamics (e.g., *Portegies Zwart et al.,* 2010), that the stars in question be gravitationally bound, or old enough to be dynamically relaxed; the former condition is often impossible to evaluate in clusters that are still embedded in their natal gas clouds, while the latter necessarily excludes the phase of formation in which we are most interested.

The argument for the importance of feedback can be made by observing that, while almost all regions of active star formation qualify as clusters by this definition, by an

age of ~10–100 m.y., only a few percent of stars remain part of clusters with stellar densities noticeably above that of the field (e.g., *Silva-Villa and Larsen,* 2011; *Fall and Chandar,* 2012). In a cluster of N stars with a crossing time t_{cross} (typically ~0.1–1 m.y. in observed clusters), two-body evaporation does not become important until an age of $(10N/\ln N)t_{cross}$ (*Binney and Tremaine,* 1987). This is ~100–1000 m.y. even for a modest cluster of N = 1000. Thus a gravitationally bound cluster will not disperse on its own over the timescale demanded by observations. However, simulations of star cluster formation that do not include feedback have a great deal of difficulty reproducing this outcome (*Bate et al.,* 2003; *Bonnell et al.,* 2003). Instead, they invariably produce bound clusters.

One might think that this problem could be avoided by positing that most stars form in gravitationally unbound gas clouds. However, such a model suffers from two major problems. First, as discussed in the chapter by Dobbs et al. in this volume, recent surveys of molecular clouds find that their typical virial ratios are $\alpha_G \approx 1$, whereas $\alpha_G > 2$ is required to render a cloud unbound. Second, *Clark et al.* (2005) find that even unbound clouds (they consider one with $\alpha_G = 4$) leave most of their stars in bound clusters. A high virial ratio means that a cloud produces a number of smaller, mutually unbound clusters rather than a single large one, but each subcluster is still internally bound and has >1000 stars. These would survive too long to be consistent with observations. Stellar feedback represents the most likely way out of this problem, as the dispersal of gas by feedback can reduce the star-formation efficiency to the point where few stars remain members of bound clusters.

A final argument for the importance of feedback comes from the problem of explaining the origin of the stellar initial mass function (IMF). As we discuss below, simulations that do not include radiative feedback tend to have problems reproducing the observed IMF, while those including it do far better (also see the chapter by Offner et al. in this volume). In the following sections, we discuss the role of feedback in solving each of these problems, and highlight both the successes and failures of current models for its operation.

1.2. A Taxonomy of Feedback Mechanisms

Before discussing individual feedback mechanisms in detail, it is helpful to lay out some categories that can be used to understand them. Although many such taxonomies are possible, we choose to break feedback mechanisms down into three categories: (1) momentum feedback, (2) "explosive" feedback, (3) and thermal feedback.

Momentum feedback is, quite simply, the deposition of momentum into star-forming clouds so as to push on the gas, drive turbulent motions within it, and, if the feedback is strong enough, to unbind them entirely. The key feature of momentum feedback, which distinguishes it from explosive feedback, is the role of radiative energy loss. The dense, molecular material from which stars form, or even

the less-dense gas of the atomic interstellar medium (ISM), is extremely efficient at radiative cooling. As a result, when stars inject energy into the ISM, it is often the case that the energy is then radiated away on a timescale that is short compared to the dynamical time of the surrounding cloud. In this case the amount of energy delivered to the cloud matters little, and the effectiveness of the feedback is instead determined by the amount of momentum that is injected, since this cannot be radiated away. As we discuss below, protostellar outflows and (probably) radiation pressure are forms of momentum feedback.

In contrast, explosive feedback occurs when stars heat gas so rapidly, and to such a high temperature, that it is no longer able to cool on a cloud dynamical timescale. In this case at least some of the energy added to the cloud is not lost to radiation, and feedback is accomplished when the hot, overpressured gas expands explosively and does work on the surrounding cold molecular material. To understand the distinction between explosive and momentum-driven feedback, consider a point source injecting a wind of material into a uniform, cold medium, and sweeping up an expanding shell of material of mass M_{sh} and radius r_{sh}. If the wind is launched with mass flux $\dot{M}_w$ at velocity v_w, and in the process of sweeping up the shell there are no radiative losses (the extreme limit of the explosive case), then after a time t the kinetic energy of the shell is $M_{sh}\dot{r}_{sh}^2 \sim \dot{M}_w v_w^2 t$. On the other hand, in the case of momentum feedback where energy losses are maximal, the momentum of the shell is $M_{sh}\dot{r}_{sh} \sim \dot{M}_w v_w t$, and its kinetic energy is $M_{sh}\dot{r}_{sh}^2 \sim \dot{M}_w v_w \dot{r}_{sh} t$. Thus without radiative losses, the kinetic energy of the shell at equal times is larger by a factor of $\sim v_w/\dot{r}_{sh}$. This is not a small number: In the example of 30 Doradus (Fig. 1), the measured velocity of the shell is ~25 km s^{-1} (*Chu and Kennicutt,* 1994), while typical launching velocities for O-star winds are >1000 km s^{-1}. Thus, when it operates, explosive feedback can be very effective. Winds from hot main-sequence stars, photoionizing radiation, and supernovae are all forms of explosive feedback.

Our final category is thermal feedback, which describes feedback mechanisms that do not necessarily cause the gas to undergo large-scale flows, but do alter its temperature. This is significant because the temperature structure of interstellar gas is strongly linked to how it fragments, and thus to the production of the IMF. Non-ionizing radiation is the main form of thermal feedback.

2. MOMENTUM FEEDBACK

2.1. Protostellar Outflows

2.1.1. Theory. Protostellar outflows are observed to be an integral part of star formation. Outflows eject a significant amount of mass from the regions around newborn stars, thereby helping to set the most important quantity for individual stars, their mass. Collectively, the outflows inject energy and momentum into their surroundings, modifying the environment in which the stars form (*Norman and Silk,*

1980; *McKee,* 1989; *Shu et al.,* 1999). Here we focus on this interaction, leaving the question of wind launching mechanisms to the chapter by Frank et al. in this volume. A key issue for outflows, as for all feedback mechanisms, is their momentum budget per unit mass of stars formed (a quantity with units of velocity), which we denote V_{out}. Note that V_{out} is not the velocity with which an individual outflow is launched; it is the total momentum carried by the outflows divided by the total mass of stars formed. It is therefore smaller than the velocity of an individual outflow by a factor equal to the ratio of the mass injected into the outflow divided by the stellar mass formed. A number of authors have attempted to estimate V_{out} from both theoretical models of outflow launching and from observed scaling relationships between outflow momenta and stellar properties. *Matzner and McKee* (2000) and *Matzner* (2007) estimate $V_{out} = 20$–40 km s^{-1}. The bulk of the momentum is produced by low-mass stars rather than massive ones, because outflow launch speeds scale roughly with the escape speeds from stellar surfaces, and the escape speeds from high-mass stars are not larger than those from low-mass stars by enough to compensate for the vastly greater mass contained in low-mass stars.

Protostellar outflow feedback is expected to be especially important wherever a large number of stars form close together in both space and time. The paradigmatic object for this type of feedback is the low-mass protocluster NGC 1333, where molecular line and infrared observations reveal numerous outflows packed closely together (*Knee and Sandell,* 2000; *Walawender et al.,* 2005, 2008; *Curtis et al.,* 2010; *Plunkett et al.,* 2013). The significance of outflow feedback in cluster formation can be illustrated using a simple estimate. Let the mass of the stars in a cluster be M_*, so the total momentum injected into the cluster-forming clump is $M_* V_{out}$. This momentum is in principle enough to move all the clump material (of total mass M_c) by a speed of

$$ v \sim \text{SFE} \times V_{out} \sim 5 \text{ km s}^{-1} \left(\frac{\text{SFE}}{0.2} \right) \left(\frac{V_{out}}{25 \text{ km s}^{-1}} \right) \qquad (1) $$

where $\text{SFE} = M_*/M_c$ is the star-formation efficiency of the clump. For typical parameters, this speed is significantly higher than the velocity dispersion of low-mass protoclusters such as NGC 1333. If all the momenta from the outflows were to be injected simultaneously, they would unbind the clump completely. If they are injected gradually, they may maintain the turbulence in the clump against dissipation and keep the stars forming at a relatively low rate over several free-fall times. This slow star formation over an extended period is consistent with the simultaneous presence of objects in all evolutionary stages, from prestellar cores to evolved class III objects that have lost most of their disks. The latter objects should be at least a few million years old, several times the typical free-fall time of the dense clumps that form NGC 1333-like clusters (*Evans et al.,* 2009).

Numerical simulations have demonstrated that outflows can indeed drive turbulence in a cluster-forming clump and maintain star formation well beyond one free-fall time. *Li and Nakamura* (2006) simulated magnetized cluster formation with outflow feedback assuming that stellar outflows are launched isotropically, and showed that the outflows drive turbulence that keeps the cluster-forming clump in quasi-equilibrium. The same conclusion was reached independently by *Matzner* (2007), who studied outflow-driven turbulence analytically. *Nakamura and Li* (2007) showed that collimated outflows are even more efficient in driving turbulence than spherical ones, because they reach large distances and larger-scale turbulence tends to decay more slowly. *Banerjee et al.* (2007) questioned this conclusion, performing simulations showing that fast-moving jets do not excite significant supersonic motions in a smooth ambient medium. However, *Cunningham et al.* (2009) showed that jets running into a turbulent ambient medium are more efficient in driving turbulent motions. Indeed, *Carroll et al.* (2009) were able to demonstrate explicitly that fully developed turbulence can be driven and maintained by a collection of collimated outflows, even in the absence of any magnetic field. Magnetic fields tend to couple different parts of the clump material together, which enables the outflows to deposit their energy and momentum in the ambient medium more efficiently (*Nakamura and Li,* 2007; *Wang et al.,* 2010).

The effects of magnetic fields and outflow feedback on cluster formation are illustrated in Fig. 2, which shows the rates of star formation in a parsec-scale clump with mass on the order of 10^3 M$_\odot$ for four simulations of increasing complexity. In the simplest case of no turbulence, magnetic field, or outflow feedback (the top left line in the figure), the clump collapses rapidly, forming stars at a rate approaching the characteristic free-fall rate (the dashed line). This rate is reduced progressively with the inclusion of initial turbulence (second solid line from top), turbulence and magnetic field (third line), and turbulence, magnetic field, and outflow feedback (bottom line). In the case with all three ingredients, the star-formation rate is kept at ~10% of the free-fall rate (the dotted line). One implication of these and other simulations is that the majority of the cluster members may be formed in a relatively leisurely manner in an outflow-driven, magnetically mediated, turbulent state, rather than rapidly in a free-fall time. Simple analytic estimates by *Nakamura and Li* (2011) suggest that outflows should be able to maintain such low star-formation rates in most of the observed clumps in the solar neighborhood.

Another implication is that outflows from low-mass stars can influence the formation of the massive stars that form in the same cluster. For example, the same simulations that show a reduction in the star-formation rate due to outflow feedback also show that outflows prevent rapid mass infall toward the massive stars that tend to reside at the bottom of the gravitational potential of protoclusters. Outflows can also have important interactions with other forms of feedback from both low- and high-mass stars, a topic we defer to section 5.1.
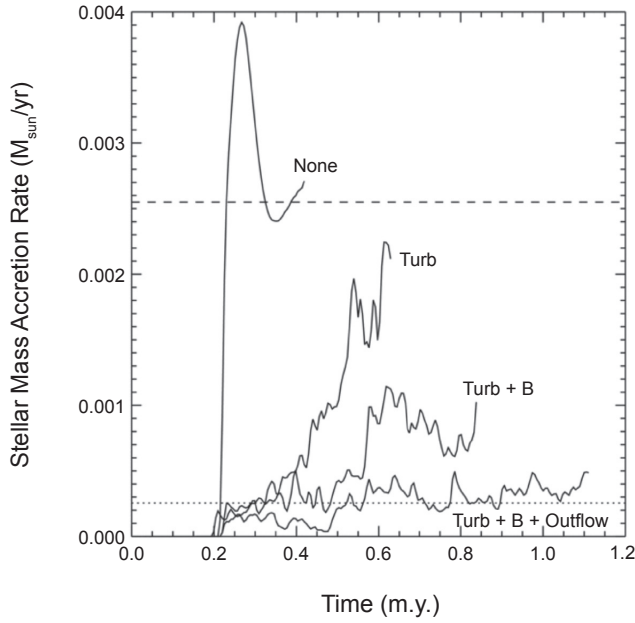
Fig. 2. The rates of star formation as a function of time for four simulations of cluster formation (adopted from *Wang et al.,* 2010). The curves from top left to bottom right are for models that include, respectively, neither turbulence nor magnetic field nor outflow feedback (line labeled "None"), turbulence only ("Turb"), turbulence and magnetic field ("Turb + B"), and all three ingredients ("Turb + B + outflow"; see text for discussion). The dashed horizontal line indicates a star-formation rate such that the depletion time t_{dep} is equal to the free-fall time t_{ff}, while the dotted line indicates a star-formation rate corresponding to $t_{dep} = 10\ t_{ff}$.

2.1.2. Observations. Several recent studies have searched for observational signatures of the outflow feedback effects described in the previous section. Even though not all studies use the same procedure to estimate the molecular outflow energetics and different studies use different methods to assess the combined impact from all outflows on the cluster gas, there are some points of consensus. One is that, in the vast majority of regions, the combined action of all outflows seems to be sufficient to drive the observed level of turbulence. The simplest method used in observational studies to determine this has been to compare the total mechanical energy of molecular outflows (i.e., the total kinetic energy of the molecular gas that has been entrained by the protostellar wind) with the turbulent energy of the cluster gas. Studies show that for a number of clusters the current total molecular outflow energy is ~30% or more of the total turbulent energy (e.g., *Arce et al.,* 2010; *Curtis et al.,* 2010; *Graves et al.,* 2010; *Duarte-Cabral et al.,* 2012), yet for other regions the total outflow energy is just 1–20% of the total turbulent energy (e.g., *Arce et al.,* 2010; *Narayanan et al.,* 2012). It is unclear to what extent these differences in outflow energy are correlated with other cloud properties. *Sun et al.* (2006) study CO(3–2) emission from different regions of Perseus, and find that

those with active star formation, such as NGC 1333, show steeper velocity power spectral indices than more quiescent regions. However, it is not clear if differences in the turbulent energy injection are the cause, and the observations themselves are at relatively low (~80″) resolution. Further study of this question is needed.

Although such simple comparisons are useful to gauge the relative importance of outflows, they do not necessarily indicate whether outflows can maintain the observed turbulence. A better way to address this is by comparing the total outflow power (L_{flow}) or mechanical luminosity (i.e., the rate at which the outflows inject energy into their surroundings through entrainment of molecular gas by the protostellar wind) with the turbulent energy dissipation rate (L_{turb}). Although there are many uncertainties associated with the estimation of both L_{flow} and L_{turb} from observations (e.g., *Williams et al.,* 2003; *Arce et al.,* 2010), it is clear that for most protostellar clusters observed thus far $L_{flow} \sim L_{turb}$ (*Williams et al.,* 2003; *Stanke and Williams,* 2007; *Swift and Welch,* 2008; *Maury et al.,* 2009; *Arce et al.,* 2010; *Nakamura et al.,* 2011a,b). The usual interpretation has been that outflows have sufficient power to sustain (or at least provide a major source of power for maintaining) the turbulence in the region.

The physical assumption behind these observational comparisons is that the gas that has been put in motion through the interaction of the protostellar wind and the ambient medium (i.e., the gas that makes up the bipolar molecular outflow) will eventually slow down and feed the turbulent motions of the cloud through some (not well understood) mechanism. However, it is unclear how efficiently outflow motions convert into cloud turbulence, and observational studies typically do not address this issue. Among the few exceptions are the studies by *Swift and Welch* (2008) and *Duarte-Cabral et al.* (2012), which use observations of ^{13}CO and $C^{18}O$ (which are much better at tracing cloud structure than the more commonly observed ^{12}CO) to investigate how outflows create turbulence. These studies show direct evidence of outflow-induced turbulence, but both conclude that only a fraction of the outflow mechanical luminosity is used to sustain the turbulence in the cloud while a significant amount is deposited outside the cloud. They also suggest that the typical outflow energy injection scale, the scale at which the outflow momentum is most efficiently injected, is around a few tenths of a parsec, which agrees with the theoretical and numerical prediction (*Matzner,* 2007; *Nakamura and Li,* 2007). However, the clouds in these studies are relatively small and host large outflows. Similar observations of larger and denser clouds are needed to further investigate if the "outflow-to-turbulence" efficiency depends on cloud environment.

We note that even though most studies show that outflows have the potential to have significant impact on the cluster environment, recent cloud-wide surveys have shown that outflows lack the power needed to sustain the observed turbulence on the scale of a molecular cloud complex (*Walawender et al.,* 2005; *Arce et al.* 2010; *Na-*

rayanan et al., 2012) or a giant molecular cloud (*Dent et al.,* 2009; *Ginsburg et al.,* 2011), with sizes of more than 10 pc. Outflows in cloud complexes and giant molecular clouds (GMCs) are mostly clustered in regions with sizes of 1–4 pc, and there are large extents inside clouds with few or no outflows. This implies that an additional energy source is responsible for turbulence on a global cloud scale. For more discussion of this topic, see the chapter by Dobbs et al. in this volume.

Several investigators have also performed observations to study the role of outflows in gas dispersal (e.g., *Knee and Sandell,* 2000; *Swift and Welch,* 2008; *Arce et al.,* 2010; *Curtis et al.,* 2010; *Graves et al.,* 2010; *Narayanan et al.,* 2012; *Plunkett et al.,* 2013). As with the work on turbulent driving, different studies use different methods to attack this problem. One common practice has been to compare the total kinetic energy of all molecular outflows with the cluster-forming clump's gravitational binding energy, with the typical result being that total outflow kinetic energy is less than 20% of the binding energy (e.g., *Arce et al.,* 2010; *Narayanan et al.,* 2012). This simple analysis seems to indicate that in most regions outflows do not have enough energy to significantly disrupt their host clouds. An equivalent way of phrasing this conclusion is that, if all the detected (current) outflow momentum were used to accelerate gas to the region's escape velocity, at most 5–10% of the clump's mass could potentially be dispersed (*Arce et al.,* 2010). This is in stark contrast with the theoretical work of *Matzner and McKee* (2000), which suggests ejection fractions of 50–70%. One possible explanation for the discrepancy is that a significant fraction of the outflow energy is deposited outside the cloud and is not detected by the observations. Another possibility is that the momentum in currently visible outflows might be only a fraction of the total momentum from all outflows throughout the life of the cloud. However, the difference between current and total momentum would need to be a factor of ~10 to reconcile observations with theory, and a more likely scenario is that outflows disperse some of the gas, while other mechanisms, such as stellar winds and UV radiation (e.g., *Arce et al.,* 2011) remove the rest. Certainly, further observations are needed in order to better understand the role of outflows in cluster gas dispersal.

Finally, we caution that most detailed observations of outflows have concentrated on relatively nearby (d < 500 pc) clusters, which, for the most part, are only forming low- to intermediate-mass stars. These regions do not accurately represent the galactic cluster population, introducing a bias. For example, the nearby regions do not reach the stellar densities or total stellar masses found in more distant regions. There have been a number of outflow observations of high-mass star-forming regions (e.g., *Beuther et al.,* 2002; *Gibb et al.,* 2004; *Wu et al.,* 2005; *Zhang et al.,* 2005; *López-Sepulcre et al.,* 2009; *Sánchez-Monge et al.,* 2013). However, such regions are typically more than 1–2 kpc away, so only the largest (and usually most powerful) outflows in each region are resolved. High an-

gular resolution is essential to untangle the emission from the numerous outflows present in high-mass star-forming regions (e.g., *Beuther et al.,* 2003; *Leurini et al.,* 2009; *Varricatt et al.,* 2010). Consequently, a complete census of outflows (especially those from low-mass stars) in these far-away clusters has been difficult with current instruments, and more detailed observations of high-mass star-forming regions are needed in order to better understand the role of outflows in clusters. Such observations will be complicated by the fact that more massive regions will contain massive stars that produce other forms of feedback, as discussed below. This will require disentangling outflows from these other effects. The best approach may be to focus on regions that are dense and massive, but are also relatively young and thus have formed few or no massive stars yet. The Atacama Large Millimeter/sub-millimeter Array (ALMA) will certainly be instrumental in conducting these studies.

2.2. Radiation Pressure

2.2.1. Theory and radiation trapping. In clusters containing massive stars, a second form of momentum feedback comes into play: radiation pressure. Radiation feedback in general consists of the transfer of both energy and momentum from the radiation field generated by stars to the surrounding gas, but in this section we shall focus on the transfer of momentum. Except for photons above 13.6 eV, this transfer is mostly mediated by dust grains. In comparison to protostellar outflows, which deliver a momentum per unit mass of stars formed $V_{out} \sim 20$–40 km s^{-1} (over a time comparable to the accretion time, ~0.1 m.y.), a zero-age stellar population drawn from a fully sampled IMF produces a radiation field of 1140 $L_{\odot}$ per $M_{\odot}$ of stars (*Murray and Rahman,* 2010), which carries a momentum per unit time per unit stellar mass $\dot{V}_{rad} \sim 24$ km s^{-1} m.y.$^{-1}$. Thus, over the time $t_{form} \sim 1$–3 m.y. that it takes a star cluster to form, the total momentum per unit stellar mass $V_{rad} = \dot{V}_{rad} t_{form}$ injected by the radiation field can be competitive with or even exceed that of the outflows.

In the immediate vicinity of forming massive stars, on scales too small to fully sample the IMF, $\dot{V}_{rad}$ can be a factor of ~10–100 larger — an individual massive star can have a light-to-mass ratio in excess of 10^4 $L_{\odot}/M_{\odot}$, a factor of 10 higher than the IMF average. Conversely, the very steep mass-luminosity relation of stars (roughly $L \propto M^{3.5}$ near 1 $M_{\odot}$, although flattening at much higher masses) ensures that radiation pressure feedback is dominated by extremely massive stars. As a result, in clusters smaller than ~10^4 $M_{\odot}$ that do not fully sample the IMF, the light-to-mass ratio is typically much smaller than the mean of a fully sampled IMF (*Cerviño and Luridiana,* 2004; *da Silva et al.,* 2012). Radiation pressure is therefore less important compared to outflows, which to first order simply follow the mass. Even the Orion Nebula cluster, the region of massive star formation nearest to the Sun, has a light-to-mass ratio well below the expected value for a fully sampled IMF (*Kennicutt and Evans,* 2012). Thus radiation feedback from stars is likely to

play a crucial role in the formation of individual high-mass stars, in the formation of massive clusters, and possibly even on galactic scales, but is likely to be unimportant in comparison to outflows in low-mass star clusters such as those closest to the Sun.

Radiation pressure begins to become significant for a population of stars once the light-to-mass ratio exceeds ~1000 $L_\odot/M_\odot$, which corresponds to a mass of ~20 $M_\odot$ for a single star (*Krumholz et al., 2009*), and ~$10^{3.5}$ $M_\odot$ for a star cluster that samples the IMF (*Cerviño and Luridiana,* 2004; *Krumholz and Thompson,* 2012, 2013). For such stars and star clusters, much of the luminosity will come in the form of ionizing photons, and thus radiation pressure and photoionization feedback will act together; we defer a more general discussion of the latter process to section 3.2. While most classical treatments of HII regions have ignored the effects of radiation pressure, recent analytic models by *Krumholz and Matzner* (2009), *Krumholz and Dekel* (2010), *Fall et al.* (2010), and *Murray et al.* (2010, 2011) have begun to include it, as did earlier models of starburst galaxies (*Thompson et al.,* 2005). Their general approach is to solve a simple ordinary differential equation for the rate of momentum change of the thin shell bounding an evolving HII region due to both gas and radiation pressure.

In this treatment the authors introduce a factor f_{trap} [called τ_{IR} in the *Murray et al.* (2010, 2011) models] to account for the boosting of direct radiation pressure force by radiation energy trapped in the expanding shell. The momentum per unit time per unit stellar mass delivered by the radiation field to the gas is $f_{trap}V_{rad}$; thus if $f_{trap} \gg 1$, then radiation pressure can be the dominant feedback mechanism almost anywhere massive stars are present. As discussed by *Krumholz and Thompson* (2012, 2013), this factor crudely interpolates between a flow driven purely by the momentum of the radiation field and one that is partly driven by a buildup of radiation energy, in analogy with the "explosive" case introduced in section 1.2. Values of $f_{trap} \gg 1$ occur if each photon undergoes many interactions before escaping, while $f_{trap} \sim 1$ corresponds to each stellar photon being absorbed only once, depositing its momentum, and then escaping. In spherical symmetry, it is straightforward to calculate f_{trap} by solving the one-dimensional equation of radiative transfer or some approximation to it (e.g., the diffusion approximation). Several authors have done this over the years, both analytically and numerically, and found $f_{trap} \gg 1$ (e.g., *Kahn,* 1974; *Yorke and Kruegel,* 1977; *Wolfire and Cassinelli,* 1986, 1987). Once one drops the assumption of spherical symmetry, however, the problem becomes vastly more complicated. As a result, the actual value of f_{trap} has been subject to considerable debate both observationally and theoretically, as we discuss below.

2.2.2. Observations of radiation pressure effects. Only a few observations to date have investigated the importance of radiation pressure feedback. *Scoville et al.* (2001) studied the central regions of M51 and found that radiation pressure from young clusters forming there exceeds their self-gravity. They proposed that this sets an upper limit on cluster masses

of ~1000 $M_\odot$. More recent work has studied the giant HII region 30 Doradus in the Large Magellanic Clouds (LMC) (*Lopez et al.,* 2011; *Pellegrini et al.,* 2011) (Fig. 1), as well as a larger sample of HII regions in the Magellanic Clouds (*Lopez et al.,* 2013). The *Lopez et al.* (2011) study finds that f_{trap} is generally small, but that nonetheless radiation pressure dominates within 75 pc of the R136 cluster at the center of 30 Doradus. In contrast, *Pellegrini et al.* (2011) argue that radiation pressure is nowhere important in 30 Doradus. (They do not consider the pressure associated with any trapped IR radiation field, and thus do not address the question of f_{trap}.) This discrepancy is more a matter of definitions than of physics. *Lopez et al.* (2011) adopt the formal definition of radiation pressure as simply the trace of the radiation pressure tensor, while *Pellegrini et al.* (2011) attempt to compute the actual force exerted on matter by radiation. These two definitions produce very different results in the optically thin interior of 30 Doradus, since in a transparent medium the force experienced by the matter can be small even if the radiation pressure exceeds the gas pressure by orders of magnitude. Regardless of this difference in definition, both sets of authors agree that, in its present configuration, warm ionized gas pressure exceeds radiation pressure at the edge of the swept-up shell of material that bounds 30 Doradus. The two studies differ, however, on how this compares to the pressure of shock-heated gas, a topic we defer to section 3.1.

2.2.3. Simulations of radiation pressure feedback. There has been much more work on simulations of the effects of radiation pressure feedback. On the scales of the formation of individual stars (see the chapter by Tan et al. in this volume for more details), *Yorke and Sonnhalter* (2002) performed two-dimensional radiation-hydrodynamic simulations, and *Krumholz et al.* (2005b, 2007b, 2009, 2010) performed three-dimensional ones. The general picture established by these simulations, illustrated in Fig. 3, is that, despite radiation force formally being stronger than gravity on the small scales studied, radiation pressure nevertheless fails to halt accretion. Gravitational and Rayleigh-Taylor (RT) instabilities that develop in the surrounding gas channel the gas onto the star system through non-axisymmetric disks and filaments that self-shield against radiation while allowing radiation to escape through optically thin bubbles in the RT-unstable flow. The radiation-RT instability has been formally analyzed, and linear growth rates calculated, by *Jacquet and Krumholz* (2011) and *Jiang et al.* (2013).

Some details of this picture have recently been challenged by *Kuiper et al.* (2011, 2012), who use a more sophisticated radiative transfer method than *Krumholz et al.* (2009). Their improved treatment of the direct stellar radiation field increases the rate at which matter is driven away from the star, and as a result the radiation-RT instability does not have time to set in before matter is expelled. While this claim seems very likely to be true as applied to the idealized simulations performed by *Kuiper et al.* (2011, 2012), it is unclear whether it would apply in the more realistic case of a turbulent or magnetized protostellar core (*Myers*

et al., 2013), or one with a disk that is gravitationally unstable as found in the *Krumholz et al.* (2009) simulations. In these situations the initial "seeds" for the instability will be much larger, and the growth to nonlinear scale presumably
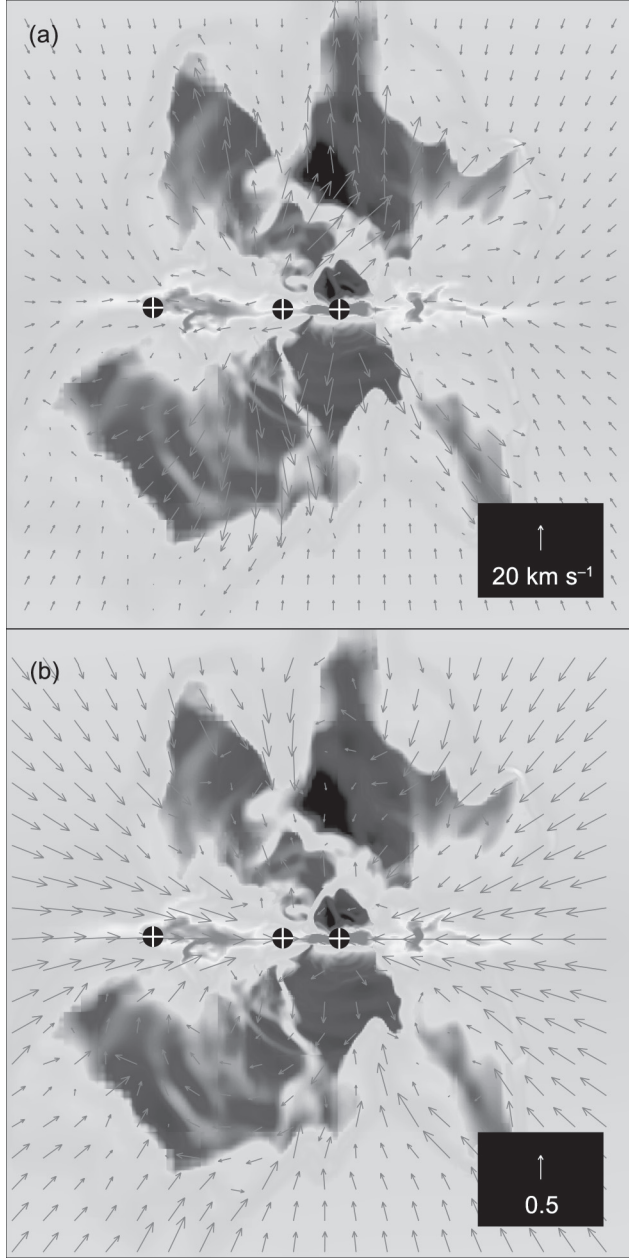
Fig. 3. Slices through a simulation of the formation of a 70-$M_\odot$ binary system, taken from *Krumholz et al.* (2009). Both panels show a region 6000 AU on a side; shades of gray show volume density on a scale from 10^{-20} to 10^{-14} g cm^{-3}, and plus signs show stars. **(a)** Arrows show the velocity; **(b)** arrows show the net radiation plus gravity force $\mathbf{f}_{rad} + \mathbf{f}_{grav}$, with the arrow direction indicating the force direction, and the arrow length scales by $|\mathbf{f}_{rad} + \mathbf{f}_{grav}|/|\mathbf{f}_{grav}|$. These slices show the simulation at a time of 1.0 mean-density free-fall times, at which point the total stellar mass is $\approx$60 $M_\odot$ and the mass of the primary is $\approx$36 $M_\odot$.

faster. Unfortunately *Kuiper et al.*'s (2011, 2012) numerical method is limited to treating the case of a single star fixed at the origin of the computational grid, and thus cannot simulate turbulent flows or provide a realistic treatment of the gravitational instabilities expected in massive star disks, which involve displacement of the star from the center of mass (*Kratter et al.,* 2010), or fragmentation of the disk into multiple stars (*Kratter and Matzner,* 2006; *Kratter et al.,* 2008; *Krumholz et al.,* 2007b; *Peters et al.,* 2010a,b, 2011). In reality the issue is likely moot in any event, as *Krumholz et al.* (2005a) show analytically and *Cunningham et al.* (2011) numerically that protostellar outflows should punch holes through which radiation can escape independent of whether radiation-RT instability occurs or not.

Much less work has been done on larger scales. A number of authors have introduced subgrid models for radiation pressure feedback, along with other forms of feedback (*Hopkins et al.,* 2011, 2012a,b; *Genel et al.,* 2012; *Agertz et al.,* 2013; *Aumer et al.,* 2013; *Stinson et al.,* 2013; *Bournaud et al.,* 2014). Others explicitly solve the equation of radiative transfer along rays emanating from stellar sources, but do not make any attempt to account for radiation that is absorbed and then reemitted (*Wise et al.,* 2012; *Kim et al.,* 2013a,b). However, none of these simulations include a fully self-consistent treatment of the interaction of the radiation field with the ISM, and as result they are forced to adopt a value of f_{trap}, either explicitly or implicitly. The outcome of the simulations depends strongly on this choice. At one extreme, some authors adopt values of $f_{trap} \gg 1$, in some cases $f_{trap} \sim 50$ (e.g., *Hopkins et al.,* 2011; *Aumer et al.,* 2013), and find that radiation pressure is a dominant regulator of star formation in rapidly-star-forming galaxies. At the other extreme, models with more modest values of f_{trap} find correspondingly modest effects (e.g., *Kim et al.,* 2013b; *Agertz et al.,* 2013). The only large-scale fully radiation-hydrodynamic simulations published thus far are those of *Krumholz and Thompson* (2012, 2013), who find that real galaxies on large scales likely have $f_{trap} \sim 1$, because radiation-RT instability reduces the efficiency of radiation-matter coupling far below the value for a laminar radiation distribution. [*Socrates and Sironi* (2013) have also argued against values of $f_{trap} \gg 1$, for somewhat different reasons.] There is some potential worry about the treatment of the direct radiation field in the *Krumholz and Thompson* (2012, 2013) models, following the points made by *Kuiper et al.* (2012). *Krumholz and Thompson* (2012, 2013) argue that if $f_{trap} \gg 1$ then the direct radiation pressure force is by definition unimportant, and thus that their treatment of radiation is adequate for investigating whether f_{trap} is indeed large. The simulations of *Jiang et al.* (2013), which use a more sophisticated treatment of radiation pressure than either *Krumholz and Thompson* (2012, 2013) or *Kuiper et al.* (2012), are qualitatively consistent with this conclusion. However, there is clearly a need for further numerical investigations with more accurate radiation-hydrodynamic methods to fully pin down the correct value of f_{trap} for use in subgrid models.

3. EXPLOSIVE FEEDBACK

3.1. Main-SequenceWinds from Hot Stars

3.1.1. Budget and relative importance. While all stars that accrete from disks appear to produce protostellar out-flows, only those with surface temperatures above ~2.5 × 10^4 K produce strong winds (*Vink et al.,* 2000). Main-sequence stars reach this temperature at a mass of ~40 $M_{\odot}$, and stars this massive have such short Kelvin-Helmholtz times that, even for very high accretion rates, they reach their main-sequence surface temperatures while still form-ing (*Hosokawa and Omukai,* 2009). As a result, hot stellar winds will begin to appear very early in the star-formation process. These winds carry slightly less momentum than the stellar radiation field (*Kudritzki et al.,* 1999); a calcula-tion using Starburst99 (*Leitherer et al.,* 1999; *Vázquez and Leitherer,* 2005) gives $\dot{V}_{msw}$ = 9 km s^{-1} m.y.$^{-1}$ per unit mass of star formed for a zero-age population.

This estimate is based on nonrotating stars of solar metallicity, using the wind prescriptions of *Leitherer et al.* (1992) and *Vink et al.* (2000). Stars of lower metallicity will have significantly lower wind momentum fluxes, due to the reduced efficiency of line-driving in a stellar atmos-phere containing fewer heavy elements (*Vink et al.,* 2001). Conversely, stellar rotation can increase the instantaneous momentum flux by a factor of a few, and the integrated momentum over the stellar lifetime by a factor of ~10, with significant uncertainty arising from the poorly known distribution of birth rotation rates (*Maeder and Meynet,* 2000, 2010; *Ekström et al.,* 2012). There is also significant uncertainty on the momentum budget at ages greater than a few million years, stemming from our poor knowledge of how exactly massive stars evolve into luminous blue variables, red and yellow supergiants, and Wolf-Rayet stars.

Despite these uncertainties, even the highest plausible stellar wind momentum estimates yield injection rates at most comparable to the stellar radiation field. Thus, if stel-lar winds represent a momentum-driven form of feedback, they should only provide a mild enhancement of radiation pressure. However, hot star winds can have terminal veloci-ties of several times 10^3 km s^{-1} (e.g., *Castor et al.,* 1975b; *Leitherer et al.,* 1992), so when they shock against one another or the surrounding ISM, the post-shock temperature can exceed ~10^7 K. At this temperature radiative cooling times are long (*Castor et al.,* 1975a; *Weaver et al.,* 1977), so shocked stellar winds might build up an energy-driven, adiabatic flow that would make them far more effective than radiation. On the other hand, they might also leak out of their confining shells of dense interstellar matter, which would greatly reduce the pressure build-up and lead to something closer to the momentum-limited case.

Whether shocked stellar wind gas does actually build up an energy-driven flow and thereby become an important feedback mechanism has been subject to considerable de-bate, and we discuss the available observational and theo-retical evidence in the next section. To frame the discussion, consider an HII region with a volume V and a pressure at its outer edge P, within which some volume V_w is occupied by X-ray emitting post-shock wind gas at pressure P_w. *Yeh and Matzner* (2012) introduce the wind parameter

$$\Omega \equiv \frac{P_w V_w}{PV - P_w V_w} \qquad (2)$$

as a measure of the relative strength of winds. The virial theorem implies that PV is what controls the large-scale dynamics, so $\Omega \gg 1$ [as expected for models such as those of *Castor et al.* (1975a) and *Weaver et al.* (1977)] indicates that the large-scale dynamics are determined primarily by winds, while $\Omega \ll 1$ [as expected in models where the post-shock wind gas undergoes free expansion (e.g., *Chevalier and Clegg,* 1985)] indicates they are unimportant. Note that P and V include any form of feedback that contributes pressure to and occupies volume within the HII region, not just the pressure and volume associated with the ~10^4 K photoionized gas (see below). Thus, Ω should be thought of as measuring the contribution of stellar winds to the total dynamical budget. As we discuss in the next section, the true value of Ω remains an open question in both observa-tions and theory.

3.1.2. Observations and theory. Observations of stellar wind feedback were revolutionized by the launch of the Chandra X-Ray Observatory, which for the first time made it possible to detect X-ray emission from the hot post-shock wind gas in HII regions (*Townsley et al.,* 2003). The sample of HII regions with X-ray measurements includes M17 and the Rosette Nebula (*Townsley et al.,* 2003), the Carina Nebula (*Townsley et al.,* 2011), the Tarantula Nebula/30 Do-radus (*Townsley et al.,* 2006; *Lopez et al.* 2011; *Pellegrini et al.,* 2011), and a few tens of smaller HII regions in the Magellanic Clouds (*Lopez et al.,* 2013). A measurement of the X-ray luminosity and spectrum can be used to infer P_w, at least up to an unknown volume filling factor. The observations conducted to date strongly rule out the largest predicted values of Ω, but the exact value is still debated. In 30 Doradus, probably the best-studied case, *Lopez et al.* (2011) and *Pellegrini et al.* (2011) report similar estimates for the pressures of 10^4-K photoionized gas and radiation, but *Pellegrini et al.*'s (2011) estimate of the X-ray-emitting gas pressure is ~2 orders of magnitude larger. Most of this discrepancy is due to differing assumptions about the volume-filling factor of the emitting gas, with *Lopez et al.* (2013) assuming it is on the order of unity and *Pellegrini et al.* (2011) arguing for a much smaller value, which would imply higher P_w but also lower V_w. *Lopez et al.*'s (2013) reported values give $\Omega \ll 1$, while the value of Ω based on *Pellegrini et al.*'s (2011) modeling is unclear because they do not report values for V_w. However, they likely obtain $\Omega \ll 1$ too, since, all other things being equal, a reduction in the filling factor tends to lower V_w more than it raises P_w.

While X-rays are the most direct way of constraining Ω, some optical and IR line ratios are sensitive to it as well (*Yeh and Matzner,* 2012; *Yeh et al.,* 2013; *Verdolini*

et al., 2013). There are significant modeling uncertainties associated with the assumed geometry, but these are quite different from the filling factor issues that hamper X-ray measurements. *Yeh and Matzner* (2012) find that available data favor $\Omega < 1$, but this is a preliminary analysis.

Several authors have also made theoretical models of wind feedback. Much of this work has treated the ISM surrounding the star as a simple uniform-density medium, and has focused on instead on the circumstellar medium, within which there can be complex interactions between components of the wind launched at different stages of stellar evolution (*Garcia-Segura et al.,* 1996a,b; *Freyer et al.,* 2003, 2006; *Toalá and Arthur,* 2011). This work, while clearly important for the study of circumstellar bubbles, offers limited insight into how wind feedback affects the process of star formation. Similarly, building on the classical *Castor et al.* (1975a) and *Weaver et al.* (1977) models, a number of authors have made increasingly sophisticated spherically symmetric models of stellar wind bubbles, including better treatments of conduction and radiative cooling (*Capriotti and Kozminski,* 2001; *Tenorio-Tagle et al.,* 2007; *Arthur,* 2012; *Silich and Tenorio-Tagle,* 2013). They find that stellar wind feedback can be dominant, but since these models necessarily exclude leakage, it is unclear how much weight to give to this conclusion.

Studies that include multi-dimensional effects in a complex, star-forming ISM are significantly fewer. *Harper-Clark and Murray* (2009) present analytic models for cold shells driven by a combination of ionized gas pressure, radiation pressure, and wind pressure, including parameterized treatments of wind leakage. These models are able to fit the observations by adopting fairly strong leakage of hot gas, and the required values of the leakage parameter suggest that hot gas is subdominant compared to other forms of feedback. Two-dimensional simulations by *Tenorio-Tagle et al.* (2007) and three-dimensional ones by *Dale and Bonnell* (2008) and *Rogers and Pittard* (2013) generally find that leakage is a very significant effect, as illustrated in Fig. 4, with a majority of the injected wind energy escaping rather than being used to do work on the cold ISM. However, even with these losses, the multi-dimensional grid-based simulations do show that a wind of hot gas is eventually able to entrain the cold ISM via Kelvin-Helmholtz instabilities and eventually remove all the cold gas from a forming star cluster. [Simulations using older formulations of smoothed particle hydrodynamics (SPH) cannot capture this effect due to their difficulties in modeling the Kelvin-Helmholtz instability (see *Agertz et al.,* 2007). Newer SPH methods can overcome this limitation (e.g., *Price,* 2008; *Read and Hayfield,* 2012; *Hopkins,* 2013), but all SPH simulations of stellar wind feedback published to date use the older methods.] These simulations, however, do not include radiation pressure or other forms of feedback, and it is unclear if winds would be dominant in competition with other mechanisms.

In addition, all the multidimensional simulations performed to date lack the resolution and the sophisticated microphysics required to handle a number of other potentially important effects. For example, the development of a turbulent interface between the cold and hot gas might greatly enhance the rate of conduction, thus lowering the temperature in the hot gas to $\sim 10^5$ K so that radiative losses via far-UV metal lines become rapid (*McKee et al.,* 1984). Another possibly important effect is mixing of dust grains into the hot gas, where, until they are destroyed by sputtering, they can remove energy via collisional heating followed by thermal radiation. In light of the continuing controversy over the importance of stellar winds, reinvestigation of these topics using modern hydrodynamic techniques is urgently needed.

3.2. Photoionization Feedback

Stars with masses ≥ 10 $M_\odot$ emit very large quantities of ionizing photons, creating ionized bubbles — HII regions. Equilibrium between heating and cooling processes inside HII regions results in them having remarkably constant temperatures of $\approx 10^4$ K and internal sound speeds of ≈ 10 km s^{-1} (*Osterbrock and Ferland,* 2006). The overpressure in the bubble causes it to expand at velocities on the order of the sound speed. In a uniform medium, this leads to the well-known Spitzer solution (*Spitzer,* 1978). As is the case with stellar winds, the interaction between the cold molecular gas and the overpressured, expanding hot gas is physically
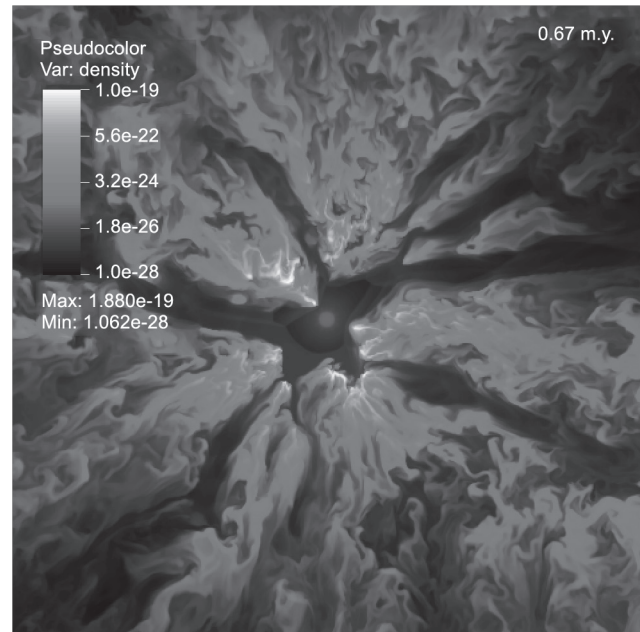
Fig. 4. Slice through a simulation of a molecular clump with hot stellar winds launched by a central star cluster. The region shown is 32 pc on a side at a time 0.67 m.y. after wind launching begins. Shades of gray show the density; the low-density channels shown in black are filled with hot, escaping wind material. Adapted from Fig. 3 of *Rogers and Pittard* (2013).

complex, and thus it is not trivial to assign a momentum budget to it and compare it to other sources of feedback. We will return to this topic below.

Observationally, HII regions are extremely bright at radio wavelengths (due to radio recombination lines and bremsstrahlung) and in the IR (due to reprocessing of stellar radiation by dust), making it possible to study them over large distances. HII regions are often divided into (ultra- or hyper-) compact and diffuse types, and this was originally thought to be an evolutionary sequence resulting from expansion. However, observations by, e.g., *Wood and Churchwell* (1989) and *Kurtz et al.* (1994) revealed that UCHII regions rarely resemble classical Strömgren spheres. Common morphologies are cometary, core-halo or shell-like, and irregular. Simulations suggest that these morphologies result from variations in the mass distribution in the immediate vicinity of the ionizing stars, and are likely to be variable over approximately a thousand years or even shorter timescales (*Peters et al.,* 2010a). *Kurtz et al.* (1999) and *Kim and Koo* (2001) found that many compact HII regions are embedded in larger diffuse ionized regions, leading *Kim and Koo* (2003) to propose that UCHII regions are dense cores embedded in champagne flows. More recent observational work has concentrated on the interaction of HII regions with IR dust bubbles (e.g., *Watson et al.,* 2008; *Deharveng et al.,* 2010; *Anderson et al.,* 2011), molecular gas (e.g., *Anderson et al.,* 2011), and stellar winds (e.g., *Townsley et al.,* 2003).

On small scales, photoionization is sometimes suggested to limit the growth of OB stars. However, *Walmsley* (1995) showed that the expansion of an HII region could be stalled or even reversed by an accretion flow. *Keto* (2003) generalized this result by showing that accretion onto an ionizing star can proceed through a gravitationally trapped HII region; observations of ionized accretion flows support this picture (*Keto and Wood,* 2006; *Klaassen and Wilson,* 2007). Simulations by *Peters et al.* (2010a,b) also found that ionizing sources were unable to disrupt accretion flows onto them until material was drained from the flows by other, lower-mass accretors. Moreover, *Hosokawa et al.* (2010, 2012) point out that accretion onto massive stars at high but not unreasonable rates causes the stars to expand, cooling their photospheres and reducing their ionizing fluxes, further easing accretion. *Klassen et al.* (2012) model the consequences of accretion-induced expansion and conclude that the shrinking of the HII region due to the drop in ionizing flux may be observable with facilities such as the Extended Very Large Array (EVLA) or ALMA. Statistical analysis of the correlation between the bolometric luminosities of massive young stellar objects and the ionizing photon fluxes required to drive the HII regions around them provides direct evidence for this effect (*Mottram et al.,* 2011; *Davies et al.,* 2011).

At larger scales, there are three major outstanding questions regarding HII regions. The first — whether they are able to trigger star formation — is discussed in section 5.2. The second is whether HII region expansion is able to drive GMC turbulence. There have been several simulations of HII region expansion in turbulent clouds (e.g., *Mellema et al.,* 2006; *Mac Low et al.,* 2007; *Tremblin et al.,* 2012b; *Dale et al.,* 2012b, 2013b), but few authors have addressed this issue in detail. *Mellema et al.* (2006) simulated the expansion of an HII region in a turbulent cloud and found that substantial kinetic energy was deposited in the neutral gas, although they did not show explicitly that this actually kept the cold gas turbulent in the sense of maintaining a self-similar velocity field over some range of scales. In their simulations of an ionizing source inside a fractal cloud, *Walch et al.* (2012) also showed that the kinetic energy of the cold gas was strongly influenced by ionization — more so than by gravity — and that a large fraction of this energy resided in random motions, which they identified as turbulence.

Gritschneder et al. (2009) simulated plane-parallel photoionization of a turbulent box and analyzed the power spectra of the velocity field both with and without the influence of feedback. They found that ionization was an efficient driver of turbulence, although with a substantially flatter power spectrum than the Kolmogorov velocity field with which the box was seeded. However, because they were irradiating the whole of one side of their simulation domain, they were driving turbulence on the largest scale available and it is not clear that this result applies more generally. In the case of point-like ionizing sources inside a large cloud, the HII regions must grow to fill a large fraction of the system volume in order for turbulent driving to be effective on the largest scales and for the turbulent cascade to operate. Semi-analytic models of GMCs including HII region feedback by *Krumholz et al.* (2006) and *Goldbaum et al.* (2011), and simulations of HII regions evolving in isolated clouds by *Walch et al.* (2012), *Dale et al.* (2012b), and *Dale et al.* (2013b) suggest that is often likely to be the case, consistent with observations that many HII regions are champagne flows.

The final question is whether HII regions can disrupt protoclusters and terminate star formation at low efficiencies. *Whitworth* (1979), *Franco et al.* (1990), *Franco et al.* (1994), *Matzner* (2002), *Krumholz et al.* (2006), and *Goldbaum et al.* (2011) found that photoionization should be effective in destroying clouds. However, these authors considered the effects of ionization on smooth clouds. The picture from recent numerical simulations of HII regions expanding in highly structured clouds is less clear. While O stars located on the edges of clouds can drive very destructive champagne flows (e.g., *Whitworth,* 1979), massive stars are usually to be found embedded deep inside clouds. In addition, molecular clouds usually possess complex density fields, and the massive stars are often located inside the densest regions. *Dale et al.* (2005) found that the influence of a photoionizing source could be strongly limited by dense large-scale structures and accretion flows. *Walch et al.* (2012) found that ionization was very destructive to $\sim 10^4$ $M_\odot$ fractal clouds on timescales of 1 m.y., but *Dale and Bonnell* (2011) and *Dale et al.* (2012b, 2013b) simulated expanding HII regions in turbulent clouds with a

range of radii (~1–100 pc) and masses (10^4–10^6 $M_\odot$) and found that the influence of ionization depends critically on cloud escape velocities. It is very effective in clouds with escape speeds well below ~10 km s^{-1}, but becomes ineffective once the escape speed reaches this value. Figure 5 shows an example. In high-escape-speed clouds, radiation pressure may dominate instead (see section 2.2).

A final caution is that, with a few exceptions (*Krumholz et al.*, 2007a; *Arthur et al.*, 2011; *Peters et al.*, 2011; *Gendelev and Krumholz*, 2012), the simulations of HII regions performed to date ignore magnetic fields, and the coupling between magnetic fields and ionizing radiation can generate unexpected effects. We discuss this further in section 5.1.

3.3. Supernovae

Supernovae represent a final source of explosive feedback. For every 100 $M_\odot$ of stars formed, ~1 star will end its life in a type II supernova; the supernovae are distributed roughly uniformly in time from ≈4 to 40 m.y. after the onset of star formation, with a slight peak during the first million years after the explosions begin (e.g., *Matzner*, 2002). Each supernova yields ~10^{51} erg, much of which ends up as thermal energy in a hot phase with a long cooling time. However, as pointed out by *Krumholz and Matzner* (2009) and *Fall et al.* (2010), supernovae are of quite limited importance on the scales of individual star clusters simply due to timescale issues. The first supernovae do not occur until roughly 4 m.y. after the onset of star formation. In comparison, the crossing time of a protocluster is $t_{cr} = 2R/\sigma$, where R and σ are the radius and velocity dispersion, respectively. Since protoclusters have virial ratios $\alpha_{vir} \approx 1$, and form a sequence of roughly constant surface density with $\Sigma \sim$ 1 g cm^{-2} (*Fall et al.*, 2010), the crossing time varies with

protocluster mass as $t_{cr} \approx 0.25(M/10^4\ M_\odot)^{1/4}$ m.y. (*Tan et al.*, 2006). Thus protoclusters have crossing times smaller than the time required for supernovae to start occurring unless their masses are $\geq 10^6\ M_\odot$. In the absence of feedback, protocluster gas clouds convert the great majority of their gas to stars in roughly a crossing time, so supernovae cannot be the dominant form of feedback in clusters smaller than ~$10^6\ M_\odot$ — such clusters would convert all of their mass to stars before the first supernova occurred, unless some other mechanism were able to delay star formation for several crossing times and allow time for supernovae to begin.

This conclusion is consistent with observations of the most massive clusters that host stars that will end their lives as supernovae. In 30 Doradus there is only one detectable supernova remnant (the bright blue spot in the lower right corner of Fig. 1) (*Lopez et al.*, 2011), and its radius is far smaller than that of the evacuated bubble. Similarly, in Westerlund 1, which has also ejected its central gas, there has been a supernova (*Muno et al.*, 2006a), but no corresponding supernova remnant has been detected (*Muno et al.*, 2006b). This is likely because the gas had already been expelled before the supernova occurred, and thus the ejecta have yet to encounter material dense enough to produce on observable shock. However, we emphasize that the conclusion that supernovae are unimportant for clusters does not apply on the larger scales of diffuse giant molecular clouds or galaxies, which have crossing times that are comparable to or significantly larger than the lifetime of a massive star.

4. THERMAL FEEDBACK

Although radiative transfer was included in some of the very earliest calculations of star formation (e.g., *Larson*, 1969), the importance of thermal feedback for star forma-
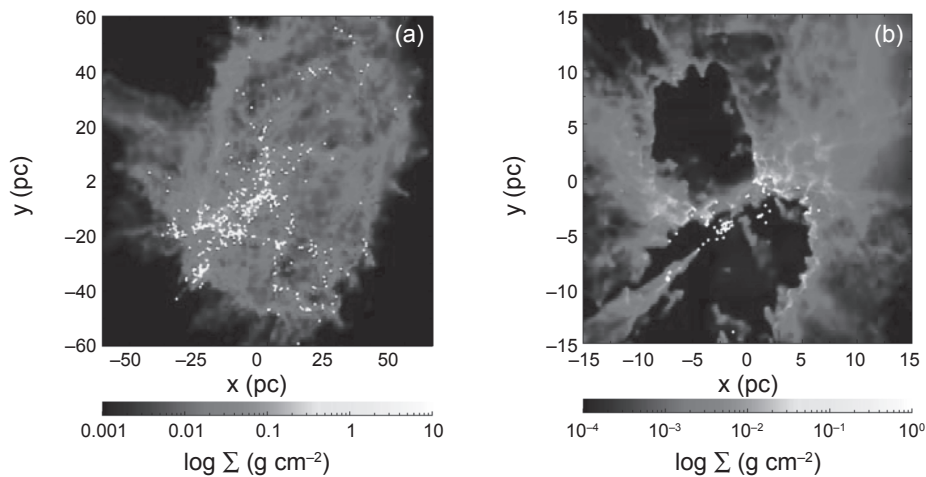
Fig. 5. Column density maps from two simulations of photoionization feedback. **(a)** Cloud with an escape speed >10 km s^{-1}, within which photoionization has done little to inhibit star formation or remove mass. **(b)** Cloud with an escape speed <10 km s^{-1}, where a majority of the mass has been ejected by photoionization feedback. Adapted from *Dale et al.* (2012b).

tion has only been recognized recently. This is true even for the case of massive star formation, where for a long time in the literature "radiative feedback" meant radiation pressure (see section 2.2), not radiative heating. This began to change in the 1980s, when three-dimensional calculations of low-mass star formation began to include radiative transfer using the Eddington approximation (*Boss,* 1983, 1984, 1986). Such calculations showed that perturbed molecular cloud cores containing several Jeans masses initially readily fragmented to form binary systems, and that dynamical collapse and fragmentation is terminated by the thermal heating after the clouds become opaque [the so-called opacity limit for fragmentation (*Low and Lynden-Bell,* 1976; *Rees,* 1976)]. However, over the past few years it has been realized that thermal feedback could play a much greater role in star formation than simply setting the minimum fragment mass.

4.1. Origin of Thermal Feedback

Thermal feedback is inevitable in the star-formation process as gravitational potential energy is converted to kinetic and thermal energy during collapse. Initially, the rate of compression of the gas is low, and the additional thermal energy is quickly radiated, resulting in an almost isothermal collapse (*Larson,* 1969). However, as the rate of collapse increases, compressional heating eventually exceeds the radiative losses (*Masunaga and Inutsuka,* 1999) and the collapse at the center of the cloud transitions to an almost adiabatic phase leading to the formation of a pressure-supported object with a mass of a few Jupiter masses and a radius of ~5 AU [the so-called first hydrostatic core (*Larson,* 1969)]. The first core accretes through a supercritical shock from which most of the accretion luminosity is radiated away (*Tomida et al.,* 2010a,b; *Commerçon et al.,* 2011b; *Schönke and Tscharnuter,* 2011). This results in heating of the surrounding gas, which, although modest, may affect fragmentation (*Boss et al.,* 2000; *Whitehouse and Bate,* 2006).

Once the center of the first hydrostatic core reaches ≈2000 K, the dissociation of molecular hydrogen initiates a second dynamical collapse, resulting in the formation of the second, or stellar, core (*Larson,* 1969; *Masunaga and Inutsuka,* 2000). The stellar core forms with a few Jupiter masses of gas and a radius of ~2 $R_\odot$. Because gravitational potential energy scales inversely with radius, the formation of the stellar core is associated with a dramatic increase in the luminosity of the protostar and significant heating to distances of hundreds of astronomical units from the stellar core (e.g., *Whitehouse and Bate,* 2006). Recent radiation hydrodynamical simulations of stellar core formation have shown that this burst of thermal feedback, due to accretion rates of ~10^{-3} $M_\odot$ yr^{-1}, which last for a few years, can be great enough to launch pressure-driven bipolar outflows (in the absence of magnetic fields) as gas and dust heated by the accretion luminosity expands and bursts out of the first hydrostatic core in which the stellar core is embedded (*Bate,* 2010, 2011; *Schönke and Tscharnuter,* 2011).

Once a stellar core forms, there are three sources of thermal feedback: (1) radiation originating from the core itself, (2) luminosity from accretion onto the star, and (3) luminosity from continued collapse of the cloud and disk accretion. For low-mass protostars (≤3 $M_\odot$) accreting at rates ≥10^{-6} $M_\odot$ yr^{-1}, accretion luminosity dominates both the intrinsic stellar luminosity (e.g., *Palla and Stahler,* 1991, 1992; *Hosokawa and Omukai,* 2009) and the luminosity of the larger-scale collapse (*Offner et al.,* 2009; *Bate,* 2012). For example, the accretion luminosity

$$L_{acc} \approx \frac{GM_* \dot{M}_*}{R_*} \qquad (3)$$

of a star of mass $M_\odot = 1$ $M_\odot$ with a radius of $R_* = 2$ $R_\odot$ (e.g., *Hosokawa and Omukai,* 2009) accreting at $\dot{M}_* = 1 \times 10^{-6}$ $M_\odot$ yr^{-1} is ≈15 $L_\odot$, whereas the luminosity of the stellar object itself is ≈1 $L_\odot$. For intermediate-mass protostars ($M_* > 3$–9 $M_\odot$), whether the accretion luminosity or the intrinsic luminosity dominates depends on accretion rate, while for masses greater than ≈9 $M_\odot$ the intrinsic stellar luminosity dominates for all reasonable accretion rates (≤10^{-3} $M_\odot$ yr^{-1}).

Several authors have considered the impact of accretion luminosity on the temperature distribution in protostellar cores of a variety of masses, both analytically and numerically (*Chakrabarti and McKee,* 2005; *Krumholz,* 2006; *Robitaille et al.,* 2006, 2007). These models show that even sub-solar-mass protostars could heat the interior of cores to temperatures in excess of 100 K to distances ~100 AU or 30 K to distances ~1000 AU. *Krumholz* (2006) points out that this could significantly inhibit fragmentation of massive cores to form stellar groups and multiple star formation in low-mass cores.

Due to the inverse radial dependence of equation (3), the luminosity from accretion onto a star will generally dominate that produced by either the accretion disk or continued collapse on larger scales. However, there are a large number of uncertainties that make accurate determination of the luminosity difficult. The evolution of the stellar core depends both on its initial structure at formation and on how much energy is advected into the star as it accretes (*Hartmann et al.,* 1997; *Tout et al.,* 1999; *Baraffe et al.,* 2009; *Hosokawa et al.,* 2011). Different assumptions give different intrinsic luminosities and stellar radii. The latter uncertainty translates into an uncertainty in the accretion luminosity. Furthermore, an unknown fraction of the energy will drive jets and outflows rather than being emitted as accretion luminosity. Furthermore, protostars may accrete much of their mass in bursts (see the chapter by Audard et al. in this volume). If this is the case, protostars may spend the majority of their time in a low-luminosity state with only brief periods of high luminosity. Thus, *Stamatellos et al.* (2011, 2012) recently argued that numerical calculations assuming continuous radiative feedback may overestimate its effects. For a detailed discussion of these issues and numerical issues related to modeling protostars with sink particles, see *Bate* (2012).

4.2. Observations of Thermal Feedback

Observations provide strong evidence for thermal feedback. The first indirect hints came from observations of a narrow CO(6–5) component around low-mass young stellar objects (YSOs), which models suggested was produced by a ~1000-AU scale region heated to ~100 K by UV photons interacting with the walls of an outflow cavity (*Spaans et al.,* 1995). More recently, several new telescopes and instruments have allowed us to obtain much larger samples to study the effects of thermal feedback on subparsec scales. Combining information on the thermal structure, thermodynamic properties, and fragmentation of cluster-forming clumps can potentially constrain the importance of thermal feedback on cluster formation (*Zhang et al.,* 2009; *Zhang and Wang,* 2011; *Longmore et al.,* 2011; *Wang et al.,* 2011).

In the vicinity of low-mass stars, *van Kempen et al.* (2009a,b) used APEX-CHAMP+ to obtain spatially resolved maps of high-J CO lines that trace warm gas around ~30 nearby sources; *van Kempen et al.* (2010) complement this with Herschel/Photodetector Array Camera and Spectrometer (PACS) spectroscopy to study the spectra in detail. *Visser et al.* (2012) and *Yıldız et al.* (2012) model the data and confirm that they are consistent with heating by a combination of stellar photons and UV produced by shocks when the jet interacts with the circumstellar medium. All these observations point to the conclusion that ~1000-AU scale, ~100-K regions are ubiquitous around the outflow cavities produced by embedded low-mass protostars.

In more massive regions, *Longmore et al.* (2011) analyzed the density and temperature structure of the massive protocluster G8.68-0.37 with an estimated mass of ≈1500 M$_\odot$. Combining Australia Telescope Compact Array (ATCA) and Submillimeter Array (SMA) observations with radiative transfer modeling, they found radial temperature profiles T ∝ r$^{-0.35}$ with temperatures of ≈40 K at distances of 0.3 pc from the cluster center. *Zhang et al.* (2009) and *Wang et al.* (2012a) used Very Large Array (VLA) ammonia observations of another massive protocluster, G28.34+0.06, and found that warmer gas seemed to be associated with outflows, but that the protostars themselves did not seem to provide significant thermal feedback on scales of 0.06 pc. The chemical species observed with Herschel also provide evidence for thermal feedback associated with outflows (*Bruderer et al.,* 2010).

By using multi-wavelength imaging, temperature maps of star-forming regions can be constructed. *Hatchell et al.* (2013) used James Clerk Maxwell Telescope (JCMT) Submillimetre Common-User Bolometer Array-2 (SCUBA-2) observations to map the temperature structure in NGC 1333, detecting heating from a nearby B star, other young IR/optical stars in the cluster, and embedded protostars. Temperatures ranged from 40 K at distances of a few thousand astronomical units from some of the more luminous stars to 20–30 K on scales of ≈0.2 pc in the northern portion of the star-forming region. They argued that heating from existing stars may lead to increased masses to the next generation of stars to be formed in the region. *Sicilia-Aguilar et al.* (2013) used multi-wavelength Herschel observations to create temperature maps of the Corona Australis region, also detecting heating from protostars on scales of thousands of astronomical units.

Therefore, from both theory and observation it is now clear that even low-mass protostars produce substantial thermal feedback on the gas and dust surrounding them. As we will discuss in the next two sections, thermal feedback may be a crucial ingredient in producing the stellar IMF.

4.3. Influence on the Initial Mass Funtion: Low-Mass End

About 15 years ago it became computationally feasible to perform hydrodynamic simulations of the gravitational collapse of molecular clouds to produce groups of protostars (e.g., *Bonnell et al.,* 1997; *Klessen et al.,* 1998; *Bate et al.,* 2003). Early simulations treated the gas either isothermally or using simple barotropic equations of state. These calculations were able to produce IMF-like stellar mass distributions, but with two major problems. First, simulations systematically over-produced brown dwarfs compared with observed galactic star-forming regions (*Bate et al.,* 2003; *Bate and Bonnell,* 2005; *Bate,* 2009a), particularly in the case of decaying turbulence (*Offner et al.,* 2008). Second, the characteristic mass of stars formed in the simulations was proportional to the initial Jeans mass (*Klessen and Burkert,* 2000, 2001; *Bate and Bonnell,* 2005; *Jappsen et al.,* 2005; *Bonnell et al.,* 2006), while there is no firm evidence for such environmental dependence in reality (*Bastian et al.,* 2010).

To explain why the characteristic stellar mass does not vary strongly with environment, several authors have suggested that it might be set by microphysical processes that cause the equation of state to deviate subtly from isothermal, e.g., a changeover from cooling being dominated by line emission to being dominated by dust emission at some characteristic density (*Larson,* 1985, 2005). Simulations using such non-isothermal equations of state show that they are capable of producing a characteristic stellar mass that does not depend on the mean density or similar properties of the initial cloud (*Jappsen et al.,* 2005). However, these models neglected the effects of stellar radiative feedback, which, as discussed above, heats the gas near existing protostars and inhibits fragmentation. Indeed, radiation-hydrodynamic simulations show that, once radiative feedback is included, the proposed non-isothermal equations of state do not provide a good description of the actual temperature structure (*Krumholz et al.,* 2007b; *Urban et al.,* 2009).

The first cluster-scale calculations to include radiative transfer (*Bate,* 2009b; *Offner et al.,* 2009; *Urban et al.,* 2010) showed that this drastically reduces the amount of fragmentation even in regions that produce only low-mass stars. As a result, the typical stellar mass is greater than without thermal feedback, greatly reducing the ratio of brown dwarfs to stars and bringing it into good agreement

with the observed galactic IMF. However, potentially of even more importance, *Bate* (2009b) also showed that radiative feedback apparently removed the dependence of the IMF on the initial Jeans mass of the cloud, and therefore could be a crucial ingredient for producing an invariant IMF. *Krumholz* (2011) took Bate's argument even further and proposed that the characteristic mass of the IMF may be linked, through thermal feedback, to a combination of fundamental constants.

More recent radiation-hydrodynamic simulations of larger clouds that produce hundreds of protostars have yielded populations of protostars whose mass distributions are statistically indistinguishable from the observed IMF (*Bate*, 2012; *Krumholz et al.*, 2012a). Figure 6 shows some example results. This led a number of authors to conclude that gravity, hydrodynamics, and thermal feedback may be the primary ingredients for producing the statistical properties of low-mass stars. However, none of the above simulations included magnetic fields.

4.4. Influence on the Initial Mass Function: High-Mass End

Thermal feedback from protostars is fundamentally a local effect, and is stronger for higher mass protostars and/or greater accretion rates (equation (3)). Therefore, it becomes even more important if the molecular cloud core has a high density and/or produces a massive protostar. In the absence of thermal feedback, a massive dense molecular cloud core is prone to fragment into many protostars since the Jeans mass scales inversely with the square root of the density. Such fragmentation typically leads to a dense cluster of protostars that evolve according to competitive accretion, resulting in a cluster with a wide range of stellar masses (e.g., *Bonnell et al.*, 2004). However, the inclusion

of thermal feedback can substantially alter this picture since the heating may be strong enough to exclude the vast majority of fragmentation, with the result that only a few massive stars are produced rather than a populous cluster (*Krumholz et al.*, 2007b). This implies that massive stars may be preferentially produced in regions with high densities (*Krumholz and McKee*, 2008; *Krumholz et al.*, 2010).

While thermal feedback can be important for reducing the level of fragmentation and producing massive stars, in some calculations it can be too dominant. *Krumholz et al.* (2011) found that as the star formation proceeds in a dense cluster-forming cloud and the thermal feedback becomes more intense, the rate of production of new protostars can decrease. Since the protostars in the cloud continue to accrete more and more mass, this can lead to a situation in which the characteristic mass of the stellar population increases with time. This means that the stellar mass distribution evolves with time, rather than always being consistent with the observed IMF as in calculations of stellar clusters forming in lower-density clouds (*Bate*, 2012). In the long term, this would result in a top-heavy IMF. Combining the effects of radiative feedback and protostellar outflows may provide a way to reduce this effect, however (see section 5.1).

Peters et al. (2010a,b, 2011) obtained a somewhat different result in their simulations, finding that radiative feedback only modestly reduced the degree of fragmentation. They term the phenomenon they observe "fragmentation-induced starvation," a process by which, if a secondary protostar manages to form in orbit around a massive protostar, it may reduce the growth rate of the massive protostar by accreting material that it would otherwise accrete. *Girichidis et al.* (2012a,b) show that fragmentation-induced starvation also occurs in more general geometries, albeit in simulations that do not include radiative feedback. The relatively
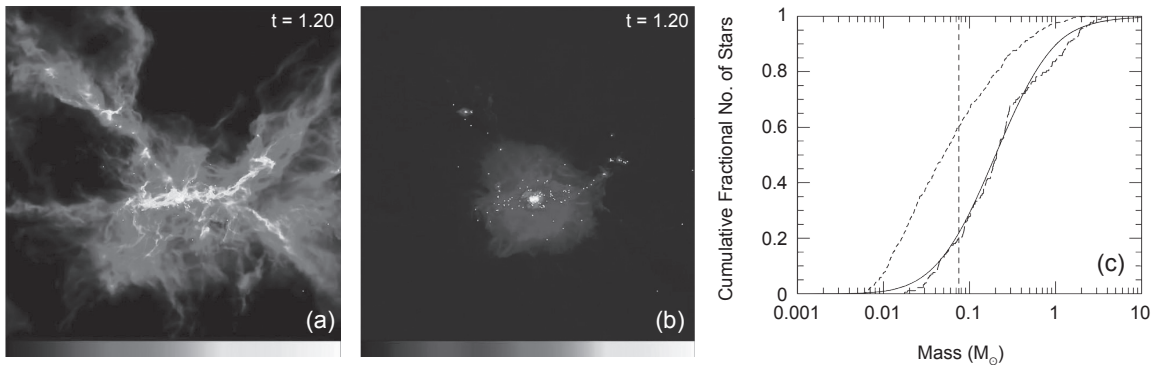
Fig. 6. Results from a radiation-hydrodynamic simulation of the formation of a star cluster in a 500-$M_\odot$ gas cloud by *Bate* (2012). **(a)** Gas column density Σ at the end of the simulation on a logarithmic scale from $-1.4 < \log \Sigma < 1.0$ with Σ in g cm^{-2}. **(b)** Density-weighted temperature on a linear scale from 9 to 50 K. **(c)** Cumulative mass distribution of the stars at the end of the simulation (dashed line), and for comparison the observed IMF [solid line (*Chabrier*, 2005)] and the mass distribution from a simulation with identical initial conditions and evolved to the same time using a barotropic equation of state [dotted line (*Bate*, 2009a)]. Figures adapted from *Bate* (2012).

modest effects of radiative feedback in the *Peters et al.* (2010a,b, 2011) simulations stands in contrast to the much stronger effects identified by *Krumholz et al.* (2011, 2012b) and *Bate* (2012).

Some of this difference may originate in the numerical method for treating radiation, with *Peters et al.* (2010a,b, 2011) using a ray-tracing method that only follows photons directly emitted by the star, while *Krumholz et al.* (2011, 2012b) and *Bate* (2012) use a diffusion method that follows the dust-reprocessed radiation but only indirectly treats direct stellar photons. However, a more likely explanation is a difference of initial conditions. *Krumholz and McKee* (2008) and *Krumholz et al.* (2010) argue that the surface density of a region is the key parameter that determines how effective radiative feedback will be, since it determines how effectively stellar radiation is trapped. In their simulations, *Krumholz et al.* (2011, 2012b) consider a region similar to the center of the Orion Nebula cluster, with a surface density $\Sigma \approx 1$ g cm^{-2} (≈ 5000 M$_\odot$ pc^{-2}), while *Bate* (2012) simulates a region with $\Sigma \approx 0.2$ g cm^{-2} (≈ 1000 M$_\odot$ pc^{-2}), similar to nearby low-mass star-forming regions such as Serpens or ρ Ophiuchus. In contrast, *Peters et al.* (2010a,b, 2011) use an initial condition with $\Sigma \approx 0.03$ g cm^{-2} (≈ 100 M$_\odot$ pc^{-2}), comparable to the surface density in giant molecular clouds averaged over >10-pc scales (see the chapter by Dobbs et al. in this volume). *Peters et al.*'s (2010a,b, 2011) surface density is low enough that their cloud is optically thin in the near-IR, and it is not surprising that radiative heating has minimal effects in such an environment, since any stellar radiation absorbed by the dust escapes as soon as it is reemitted, rather than having to diffuse outward and heat the cloud in the process.

Simultaneous observations of fragmentation and temperature distribution in cluster-forming clumps can provide a key observational test of the numerical results. Recent high-angular-resolution observations of dense, massive IR dark clouds, precursors to cluster-forming regions, have begun to detect massive cores at the early phases of cluster formation (*Rathborne et al.,* 2008; *Zhang et al.,* 2009; *Bontemps et al.,* 2010; *Zhang and Wang,* 2011; *Wang et al.,* 2011, 2012b; *Longmore et al.,* 2011). Indeed, these cores contain masses at least a factor of 10 larger than the Jean mass (*Zhang et al.,* 2009). However, they do not appear to lie in the high-temperature sections of the clump (*Wang et al.,* 2012b), which appears to conflict with numerical simulations. Future observations of larger samples of massive cluster-forming clumps will provide a statistical trend that further constrains the role of thermal feedback to the formation of massive stars (see section 6.1).

5. PUTTING IT ALL TOGETHER

5.1. Interactions Between Feedback Mechanisms

5.1.1. Combined effects of multiple mechanisms. In the preceding sections, we have discussed the effects of various different types of feedback individually. However, in

reality, feedback mechanisms frequently act simultaneously. For low-mass star formation, the dominant mechanisms are thought to be protostellar outflows and thermal feedback. Radiation pressure is negligible and supernovae do not occur. Photoionization will only affect the immediate vicinities of protostars, although it may be crucial for the erosion of protoplanetary disks (*Hollenbach et al.,* 1994; *Yorke and Welz,* 1996; *Richling and Yorke,* 1997; *Clarke et al.,* 2001). In contrast, the feedback from high-mass protostars involves all the above mechanisms.

Both analytic and numerical investigations of multiple mechanisms are few. *McKee et al.* (1984) considered the interaction of a stellar wind and photoionization with a clumpy medium, and concluded that the photoevaporation of clumps would control the dynamics, either by creating an ionized medium that would pressure-confine the wind or by providing a mass load that would limit its expansion. *Krumholz et al.* (2005a) showed that protostellar outflows would significantly weaken the effects of radiation pressure feedback by creating escape routes for photons. *Cunningham et al.* (2011) confirmed this prediction with simulations, and also showed that focusing of the radiation by the outflow cavity prevents the formation of radiation-pressure-driven bubbles and the associated Rayleigh-Taylor instabilities seen in earlier calculations (*Krumholz et al.,* 2009).

Hansen et al. (2012) investigated the combined effects of radiative transfer and protostellar outflows on low-mass star formation. As the outflows reduce the accretion rates of the protostars, they also reduce their masses and luminosities and hence the level of thermal feedback. They found that the outflows did not have a significant impact on the kinematics of the star-forming cloud, but the calculations did not include magnetic fields. In section 4.4, we mentioned that *Krumholz et al.* (2011) found that in massive dense star-forming clouds, thermal feedback could be so effective at inhibiting fragmentation that it led to a top-heavy IMF. However, *Krumholz et al.* (2012a) showed that this "overheating problem" could be reduced by including the effects of large-scale turbulent driving and protostellar outflows, since both of these processes lower protostellar accretion rates and thus the effects of thermal feedback. This is one case where the details of, and uncertainties in, accurately determining the luminosities of protostars (see section 4.1) can play a crucial role in the outcome of star formation.

A number of authors have also simulated the interaction of stellar winds with photoionized regions (e.g., *Garcia-Segura et al.,* 1996a,b; *Freyer et al.,* 2003, 2006; *Toalá and Arthur,* 2011). However, these simulations generally begin with a single star placed in a uniform, non-self-gravitating medium. While this setup is useful for studying the internal dynamics of wind bubbles, it limits the conclusions that can be drawn about how the feedback affects the formation of star clusters, where the surrounding medium is highly structured and strongly affected by gravity.

5.1.2. Feedback, turbulence, and magnetic fields. Some feedback effects are enhanced by the presence of turbulence and/or magnetic fields, while others are reduced. For

example, *Banerjee et al.* (2007) examined jets propagating into a quiescent medium and concluded that they do not drive supersonic turbulence, while *Cunningham et al.* (2009) shows that jets propagating into a preexisting turbulent medium could inject energy into the turbulence, thus potentially allowing outflows to sustain existing turbulence in a star-forming region. It has been noted, however, that the velocity power spectrum of the turbulence generated by outflows in magnetized clouds may be slightly steeper than that generated by isotropic forcing (*Carroll et al.,* 2009).

By themselves, stronger magnetic fields have been shown to reduce the star-formation rate in molecular clouds (*Nakamura and Li,* 2007; *Price and Bate,* 2008, 2009). However, magnetic fields can also interact with feedback effects in subtle ways. We already discussed (section 2.1.1) how magnetic fields enhance the effects of protostellar outflows by raising the efficiency with which they deposit their energy in clouds. *Gendelev and Krumholz* (2012) demonstrated a similar magnetic enhancement in the effects of photoionization feedback. On the other hand, *Peters et al.* (2011) investigate the interaction of magnetic fields with ionizing radiation on smaller scales, and find that ionizing radiation tends to make it harder for massive stars to drive collimated magnetized outflows, because the pressure of the photoionized gas disrupts the magnetic tower configuration that can drive outflows from lower mass stars.

In a similar vein, while it has been known for some time that magnetic fields alone reduce fragmentation in collapsing gas (e.g., *Hennebelle et al.,* 2011), they also appear to greatly enhance the effects of thermal feedback. *Commerçon et al.* (2010, 2011a) and *Myers et al.* (2013) find that magnetic fields provide an efficient mechanism for angular momentum transport and thus tend to increase accretion rates onto forming stars. This in turn raises their accretion luminosities, and thus the strength of thermal feedback. Moreover, thermal feedback and magnetic fields work well in combination to reduce fragmentation in both low- and high-mass star-formation calculations. For low-mass clusters, *Price and Bate* (2009) found that thermal feedback inhibits fragmentation on small scales, while magnetic fields provide extra support on large scales. The result is that the combination of magnetic fields and thermal feedback is much more effective than one would naively guess. For massive cores, *Commerçon et al.* (2010, 2011a) find a similar effect operating at early times, up to the formation of a Larson's first core. However, they are unable to address the question of fragmentation at later times.

Myers et al. (2013) use a subgrid stellar evolution model that allows them to run for much longer times than *Commerçon et al.* (2010, 2011a), and find that thermal feedback inhibits fragmentation in the dense central regions, while magnetic fields inhibit it in the diffuse outer regions. They find that strong magnetic fields and thermal feedback in massive dense cores make it very difficult to form anything other than a single massive star or, perhaps, a binary. Figure 7 illustrates this effect. It shows the results of three simulations by *Myers et al.* (2013) using identical resolution and initial conditions, one with magnetic fields but no radiation, one with radiation but no magnetic fields, and one with both radiation and magnetic fields. The run with both forms many fewer stars than one might naively have guessed based on the results with radiation or magnetic fields alone.

These results are in contrast to those of *Peters et al.* (2011), who also include both radiation and magnetic fields, but find only a modest reduction in fragmentation. As discussed in section 4.4, this is likely a matter of initial conditions: *Commerçon et al.* (2010, 2011a) and *Myers et al.* (2013) consider dense prestellar cores with surface density $\Sigma \approx 1$ g cm^{-2} [chosen to match observed IR dark cloud cores (*Swift,* 2009)], while *Peters et al.* (2011) simulate much more diffuse regions with $\Sigma \approx 0.03$ g cm^{-2}, and is not clear if their calculations ever evolve to produce the sorts of structures from which *Commerçon et al.* (2010, 2011a) and *Myers et al.* (2013) begin.

The combined effects of magnetic fields and thermal feedback can even modify star-formation rates. Thermal feedback by itself reduces star-formation rates by at most tens of percents (*Bate,* 2009b, 2012; *Krumholz et al.,* 2010), but adding magnetic fields can reduce the star-formation rate in low-mass clusters by almost an order of magnitude over purely hydrodynamic collapse (*Price and Bate,* 2009) and significantly more than magnetic fields alone.

5.2. Triggering

Thus far we have primarily focused on negative feedback, in the sense of restraining or terminating star formation. However, it is also possible for feedback to be positive, in the sense of promoting or accelerating feedback. The statistical arguments outlined in section 1.1 would tend to suggest that negative feedback must predominate, but this does not necessarily imply that positive feedback never occurs or cannot be important in some circumstances.

Positive feedback is usually referred to as triggered or induced star formation. This phrase can mean increasing the star-formation rate, increasing the star-formation efficiency, or increasing the total number of stars formed. These definitions can all be applied locally or globally. *Dale et al.* (2007) draw a distinction between weak triggering — temporarily increasing the star-formation rate by inducing stars to form earlier — and strong triggering — increasing the star-formation efficiency by causing the birth of stars that would not otherwise form. They note that it may be very difficult for observations to distinguish these possibilities.

Analytic studies by *Whitworth et al.* (1994a) suggest that the gravitational instability operating in swept-up shells driven into uniform gas by expanding Hɪɪ regions or wind bubbles should be an efficient triggering process. *Whitworth et al.* (1994b) extended this work to show that this process should result in a top-heavy IMF, a result also found in simulations of fragmenting shells by *Wünsch et al.* (2010) and *Dale et al.* (2011). This raises the intriguing prospect of star formation as a self-propagating process (e.g., *Shore,*
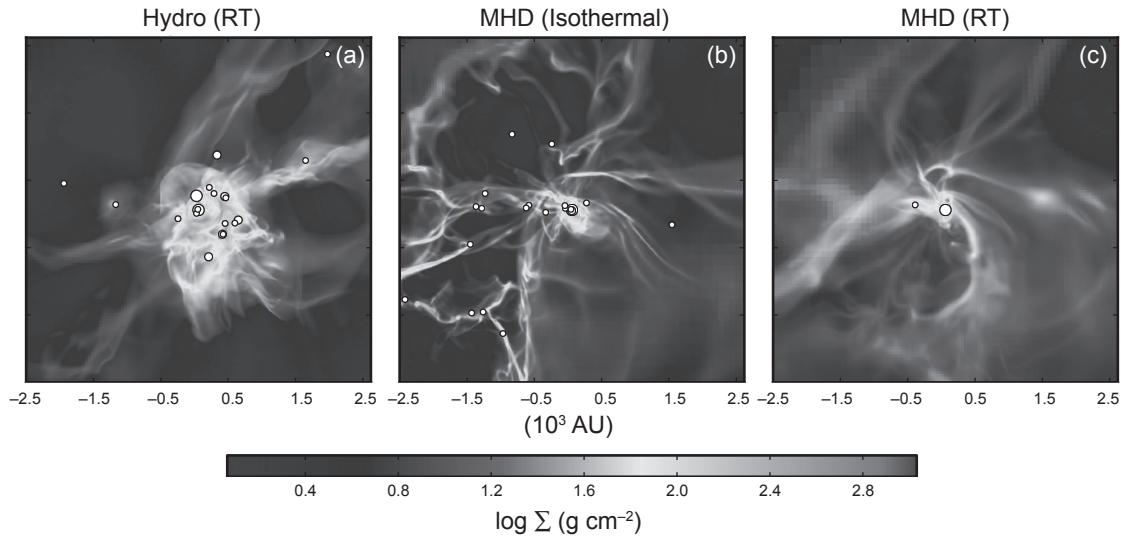
Fig. 7. Results from three simulations by *Myers et al.* (2013). The color scale shows the column density, and white circles show stars, with the size of the circle indicating mass: <1 $M_\odot$ (small circles), 1–8 $M_\odot$ (medium circles), and >8 $M_\odot$ (large circles). **(a)** Simulation including radiative transfer (RT) but no magnetic fields; **(b)** simulation with magnetic fields but no radiative transfer; **(c)** simulation with both radiative transfer and magnetic fields. All runs began from identical initial conditions, and have been run to 60% of the free-fall time at the initial mean density.

1981, 1983). However, simulations of ionizing feedback in fractal (*Walch et al.,* 2013) and turbulent clouds (*Dale et al.,* 2007, 2012a, 2013a; *Dale and Bonnell,* 2012) suggest that this is not the case. They find that, while ionization feedback can modestly change the rate, efficiency, and number of stars, it does not significantly alter the IMF.

Pillars or "Elephant Trunks" are a widespread and distinctive feature of star-forming regions and have often been invoked as signposts of triggering (e.g., *Smith et al.,* 2000, 2005; *Billot et al.,* 2010). *Williams et al.* (2001), *Miao et al.* (2006), *Gritschneder et al.* (2010), *Mackey and Lim* (2011), *Tremblin et al.* (2012a,b), and *Walch et al.* (2013) have simulated pillar formation in a wide variety of initial conditions and provide several plausible mechanisms for their origins. However, it is not clear to what extent these morphological features are actually indicative of triggered star formation.

There is also large body of literature on the induced collapse of initially stable density configurations, such as Bonner-Ebert spheres, by winds or by HII regions, known as radiation-driven implosion (e.g., *Sandford et al.,* 1982, 1984; *Klein et al.,* 1983; *Bertoldi,* 1989; *Bertoldi and McKee,* 1990; *Kessel-Deynet and Burkert,* 2003; *Bisbas et al.,* 2011). This process is able to produce not only single stars, but small groups, and since the initial conditions are stable by construction, this is a good example of strong triggering.

Establishing the occurrence of triggered star formation analytically or numerically is relatively straightforward. One can use either initial conditions that are stable in the absence of feedback, as in the radiation-driven implosion simulations, or, for more complex initial conditions, control simulations without feedback. Detecting triggering in observed systems is much more difficult, since neither of these paths are open to the observer. Instead, observers must search for circumstantial evidence for triggering. Examples of such attempts in the literature include surveys of young stars near bubbles, ionization fronts, or bright-rimmed clouds (e.g., *Urquhart et al.,* 2007; *Deharveng et al.,* 2008; *Snider et al.,* 2009; *Smith et al.,* 2010) or pillars, campaigns to find clusters elongated toward feedback sources or showing strong age gradients in young stars (e.g., *Sugitani et al.,* 1995; *Chauhan et al.,* 2009; *Getman et al.,* 2012), and searches for regions of unusually high star-formation rate or efficiency (e.g., *Bisbas et al.,* 2011). In these observational campaigns, the standard practice has been to claim evidence for triggered star formation whenever there are coherent structures within which the stellar age differences are smaller than the crossing time of the cloud structure. Generally such structures are compressed shells of molecular gas with tens of parsec radii, such as the CepOB2 bubble (*Patel et al.,* 1998) or the MonR2 GMC (*Xie and Goldsmith,* 1994).

This approach must be treated with caution, because star formation correlates with the presence of dense gas on parsec scales even in the absence of obvious feedback or triggering (*Heiderman et al.,* 2010; *Gutermuth et al.,* 2011). Thus one expects to find correlations between YSOs and nebulosity features even in the absence of triggering. For evidence of triggering to be convincing, one must show that

the correlation between star formation and feedback-driven features is in excess of what one would expect simply from the baseline correlation of YSOs and dense gas. For example, in some cases the ratio of YSO mass to molecular gas mass is far higher than one normally finds in active star-forming regions (e.g., *Getman et al.,* 2009). However, even in such cases it is unclear whether the enhancement is a matter of positive feedback (enhanced star formation raising the stellar mass) or negative feedback (ablation of gas reducing the gas mass without creating any additional stars).

The contribution of triggered star formation to the global star-formation rate is unclear. Most GMCs have uniformly low star-formation efficiencies (*Evans et al.,* 2009), showing no obvious correlation with numbers of OB stars or signs of feedback such as bubbles. *Kendrew et al.* (2012) and *Thompson et al.* (2012) use statistical correlations between large catalogs of bubbles and young stellar objects to infer that triggered star formation may contribute at most tens of percents to the galactic population of massive stars. Such a small variation is well within the cloud-to-cloud scatter in star-formation efficiency seen by *Evans et al.* (2009); indeed, it is smaller than the typical observational uncertainty on the star-formation rate, particularly within a single cloud. Similarly, simulations by *Dale et al.* (2012a, 2013a) imply that, while triggering certainly does occur, it is overwhelmed by negative feedback on the scale of GMCs.

Ultimately, quantifying the sizes and timescales for the destructive influences of feedback is essential; outside these zones of negative influence, large-scale effects from feedback may indeed turn positive, especially in aggregate with other moderately nearby feedback sources. Are these aggregate effects truly triggering, or are they simply the source of the large-scale turbulence that drives the creation of the next generation of star-forming molecular material?

6. FUTURE PROSPECTS

6.1. Observations

In order to place more stringent constraints on how feedback affects the star- and cluster-formation process, new observations must tackle the problem on two fronts. Naturally, we must continue to push to observe statistically significant samples of ever more extreme (and more distant) environments as they come within reach of new facilities across the electromagnetic (EM) spectrum. In addition, we must endeavor to improve our understanding of star formation within nearby, low-feedback environments in order to set an interpretive framework that will be essential for determining the net effect of more extreme feedback. In both cases, characterization of the properties and kinematics of star-forming gas and the forming stars themselves will be essential.

High-angular-resolution observations of protocluster-forming regions have revealed fragmentation of dense molecular gas at spatial scales of $<10^3$ AU (*Rathborne et al.,* 2008; *Zhang et al.,* 2009; *Bontemps et al.,* 2010; *Zhang*

and Wang, 2011; *Wang et al.,* 2011, 2012a; *Longmore et al.,* 2011; *Palau et al.,* 2013). Despite limited sensitivity and dynamic range, these observations provided valuable snapshots of density and temperature distributions of the star-forming gas. The next generation of interferometers such as ALMA will provide even more detailed images of density distribution and linewidth of star-forming cores in protocluster-forming molecular clumps. At the same time, the temperature distribution within the molecular clump can be readily obtained from observations with the Karl Jansky VLA (e.g., *Wang et al.,* 2008, 2012a). The combined information will constrain the thermal dynamic properties and fragmentation of cluster-forming clumps, providing direct information on the initial physical properties of molecular gas that gives rise to a stellar cluster.

A survey of nearby clusters, within ~500 pc, using existing millimeter interferometers [e.g., Combined Array for Research in Millimeter-wave Astronomy (CARMA) (see *Plunkett et al.,* 2013)] or heterodyne receiver arrays in (sub)-millimeter (single-dish) telescopes [e.g., SEQUOIA on Large Millimeter Telescope (LMT) or the 64-pixel array Supercam on Submillimeter Telescope (SMT)] allow for efficient mapping of outflows using different CO transition lines. Even though in many cases the angular resolution will not be enough to resolve individual outflows in regions with a high density of protostars, these observations will be necessary to obtain total molecular outflow energetics and compare them with cloud energy and gas distribution for a large sample of clusters. Observations of these regions should also include maps of higher (column) density tracers, such as ^{13}CO and $C^{18}O$, in order to investigate the impact of outflows and winds in the cloud structure and turbulence.

In the near future, when ALMA is completed and on-the-fly (OTF) mapping becomes available, it will be feasible to conduct studies similar to the ones described above for a (larger) sample of clusters (within about 10 kpc) that is representative of the galactic cluster population. High-resolution ALMA observations of massive (far-away) clusters will also help in studying the impact of compact H$_{\rm II}$ regions on the surrounding molecular cloud. In addition, multi-epoch VLA continuum observations of compact H$_{\rm II}$ regions will allow measurement of the expansion velocity of the ionized bubble, and in concert with multi-wavelength data, will place constraints on the impact of winds and radiation pressure on the surrounding cluster environment. However, these observations may be complicated by the fact that, at least during the hypercompact stage, some H$_{\rm II}$ regions are observed to shrink rather than expand (*Galván-Madrid et al.,* 2008), likely as a result of the motions of dense material near the ionizing source causing part of the H$_{\rm II}$ region to be shadowed (*Galván-Madrid et al.,* 2011).

At larger scales, OTF observations using heterodyne receiver arrays in millimeter single-dish telescopes will allow fast mapping of molecular gas that has been swept-up by bubbles and signal-to-noise (SNR) in high-mass star-forming regions. In lower-density regions, where there is little or no molecular gas, large-scale galactic H$_{\rm I}$ surveys

with Square Kilometre Array (SKA) precursor telescopes, like the Galactic Australian Square Kilometre Array Pathfinder (GASKAP) (*Dickey et al.,* 2013), will provide useful information on the effects of stellar feedback on the low-density outskirts of clusters.

Confidently obtaining the census of low-mass young stars forming in more diverse feedback-affected environments is essential to establishing correlations between feedback sources (e.g., their nature, position, and intensity) and changes in star-gas column density correlation or other aspects of the star-formation process. Given the simultaneous needs of moderate to high extinction penetration and membership isolation from field stars, IR and X-ray imaging capabilities remain the central means for identifying YSOs. Recent IR YSO membership surveys with Spitzer have considerably expanded our knowledge of YSOs in the nearest kiloparsec. However, they are limited in their ability to discern members projected on bright nebulosity, thus only a relatively narrow range of galactic environments have been thoroughly searched for forming stellar content throughout the stellar mass range (*Allen et al.,* 2007; *Evans et al.,* 2009; *Gutermuth et al.,* 2009; *Megeath et al.,* 2012).

X-ray observations, particularly deep and high-resolution imaging with Chandra, have proven effective at bypassing the nebulosity limitations of IR surveys, detecting substantial numbers of YSOs in particularly IR-bright high-mass star-forming regions. X-ray emission from YSOs is generally considered to be a product of magnetic field activity, and thus not strongly correlated with the presence of a disk (*Feigelson et al.,* 2007). The resulting YSO census derived from X-ray imaging therefore trades the disk bias of IR surveys for a broad completeness decay as a function of luminosity, as stochastic flaring events of gradually increasing strength, and therefore rarity, are required to detect lower-mass sources with smaller quiescent luminosities.

In the near term, improving capabilities in adaptive optics on ever-larger-aperture groundbased optical and near-IR telescopes will facilitate other means of young stellar membership isolation, both via facilitating high throughput spectroscopy as well as yielding sufficient astrometric precision for proper motion characterization (e.g., *Lu et al.,* 2013). Looking further ahead, the considerable improvement in angular resolution and sensitivity at near- and mid-IR wavelengths afforded by the James Webb Space Telescope (JWST) will dramatically improve the contrast between nebulosity and point sources in Milky Way star-forming regions, enabling Spitzer-like mid-IR YSO surveys out to much greater distances and in regions influenced by much more significant feedback sources. The resulting censuses of young stars with IR excess will reach well down the stellar mass function in regions found both within the Molecular Ring as well as toward the outskirts of the Milky Way. Unfortunately, next-generation X-ray space telescopes of similar angular resolution and better sensitivity relative to Chandra [e.g., the All-Wavelength Extended Groth Strip International Survey (AEGIS), Advanced X-ray

Spectroscopic Imaging Observatory (AXSIO), and Square Meter Arcsecond Resolution X-ray Telescope (SMART-X)] remain in the planning phase for launch on a time frame outside the scope of this review.

6.2. Simulations and Theory

In the area of simulations and theory, in the next few years we can expect improvements in several areas. The first need that should be apparent from the preceding discussion is for simulations that include a number of different feedback mechanisms, and that can assess their relative importance. As of now, there are simulations and analytic models addressing almost every potentially important form of feedback: pre-main-sequence outflows, main-sequence winds, ionizing radiation, non-ionizing radiation, radiation pressure, and supernovae. However, no simulation or model includes all of them, and only a few include more than one. Moreover, many simulations including feedback do not include magnetic fields. As discussed in section 5.1, interactions between different feedback mechanisms, and between feedback and preexisting turbulence and magnetic fields, are potentially important, but remain largely unexplored.

This limitation is mostly one of code development. Designing and implementing the numerical methods required to treat even one form of feedback in the context of an adaptive mesh refinement, smoothed particle hydrodynamics, or other code capable of the high dynamic range required to study star formation requires an effort lasting several years. As a result, no one code includes treatments of all the potentially important mechanisms. However, that situation is improving as code development progresses, and the pace of development is increasing as at least some of the remaining work involves porting existing techniques from one code to another, rather than developing entirely new ones. By the time of the next Protostars and Planets conference, it seems likely that there will be more than a few published simulations that include magnetohydrodynamics (MHD), protostellar outflows, main-sequence winds, and multiple radiation effects, including pressure and heating by both ionizing and non-ionizing photons. There are also likely to be improvements in the numerical techniques used for many of these processes, particularly radiative transfer, where it seems likely that in the next few years many codes will be upgraded to use variable Eddington tensor methods (e.g., *Davis et al.,* 2012; *Jiang et al.,* 2012) or other high-order methods such as S_n transport.

A second major area in need of progress is the initial conditions used in simulations of star-cluster formation. At present, most simulations begin with highly idealized initial conditions: either spherical regions that may or may not be centrally concentrated, or turbulent periodic boxes. In simulations without feedback, *Girichidis et al.* (2011, 2012a,b) show that the results can depend strongly on which of these setups is used. For simulations with feedback, those that run long enough and contain forms of feedback such

that they are able to reach a statistical steady state are probably fairly insensitive to the initial conditions. For the vast majority of simulations, though, particularly those where gas expulsion is rapid and occurs at most ~1 dynamical time after the onset of star formation, the initial conditions likely matter a great deal. In reality, the dense regions that form clusters are embedded within larger giant molecular clouds, which are themselves embedded in a galactic disk. They likely begin forming stars while they are still accreting mass, and the larger environments that are missing in most simulations can provide substantial inputs of mass, kinetic energy, and confining pressure. Simulations that include both the formation of a cloud and feedback have begun to appear in the context of studies of GMCs on larger scales (e.g., *Vázquez-Semadeni et al.,* 2010), and there is clearly a need to extend this approach to the smaller, denser scales required to study the formation of star clusters.

A third, closely related problem is that the current generation of simulations usually explore a very limited range of parameters — for example, only a single cloud mass and density, or a single magnetic field strength or orientation. As a result, it is difficult to draw general conclusions, particularly when results differ between groups. For example, *Wang et al.* (2010) find that including protostellar outflows dramatically reduces the star-formation rate in their simulations of cluster formation, while *Krumholz et al.* (2012b), using essentially the same prescription to model outflows, find that the effects on the star-formation rate are much more modest. Is this because *Wang et al.*'s (2010) simulations include magnetic fields and those of *Krumholz et al.* (2012b) do not? Because Krumholz et al.'s simulations include radiation and *Wang et al.*'s (2010) do not? Or because Wang et al. simulate a region modeled after a relatively low-density region like NGC 2264, while *Krumholz et al.* (2012b) choose parameters appropriate for a much-higher-density region like the core of the Orion Nebula cluster? Since each paper simulated only a single environment, the answers remain unknown. While there are analytic models that provide some guidance as to which feedback mechanisms might be important under what conditions (e.g., *Fall et al.,* 2010), there are precious few parameter studies. [See *Krumholz et al.* (2010), *Myers et al.* (2011), and *Dale et al.* (2013b) for some of the few exceptions.] This will need to change in the coming years.

All these advances are likely to require fundamental changes in the algorithms and code architecture used for numerical simulations of star-cluster formation. Using present algorithms, parallel simulations of star-cluster formation that go to resolutions high enough to (for example) resolve fragmentation to the IMF, and that include even one or two feedback mechanisms, often require many months of run time. Adding more physical processes, or more accurate treatments of the ones already included, will only exacerbate the problem. Part of the problem is that the techniques currently in use do not scale particularly well on modern massively parallel architectures. This is partly a matter

of physics: The problem of star formation is inherently computationally difficult due to the wide range of time and spatial scales that must be treated. However, it is also partly a matter of code design: Few modern multi-physics codes have been ported to hybrid threaded/message-passing architectures, and even fewer have been optimized to run on GPUs or similar special-purpose hardware. In addition to improving the physics in our codes, a great deal of software engineering will be required to meet the goals laid out above in time for the next Protostars and Planets conference.

REFERENCES

Agertz O. et al. (2007) *Mon. Not. R. Astron. Soc., 380,* 963.
Agertz O. et al. (2013) *Astrophys. J., 770,* 25.
Allen L. et al. (2007) In *Protostars and Planets V* (B. Reipurth et al., eds.), pp. 361–376. Univ. of Arizona, Tucson.
Anderson L. D. et al. (2011) *Astrophys. J. Suppl., 194,* 32.
Arce H. G. et al. (2010) *Astrophys. J., 715,* 1170.
Arce H. G. et al. (2011) *Astrophys. J., 742,* 105.
Arthur S. J. (2012) *Mon. Not. R. Astron. Soc., 421,* 1283.
Arthur S. J. et al. (2011) *Mon. Not. R. Astron. Soc., 414,* 1747.
Aumer M. et al. (2013) *Mon. Not. R. Astron. Soc., 434,* 3142.
Banerjee R. et al. (2007) *Astrophys. J., 668,* 1028.
Baraffe I. et al. (2009) *Astrophys. J. Lett., 702,* L27.
Bastian N. et al. (2010) *Annu. Rev. Astron. Astrophys., 48,* 339.
Bate M. R. (2009a) *Mon. Not. R. Astron. Soc., 392,* 590.
Bate M. R. (2009b) *Mon. Not. R. Astron. Soc., 392,* 1363.
Bate M. R. (2010) *Mon. Not. R. Astron. Soc., 404,* L79.
Bate M. R. (2011) *Mon. Not. R. Astron. Soc., 417,* 2036.
Bate M. R. (2012) *Mon. Not. R. Astron. Soc., 419,* 3115.
Bate M. R. and Bonnell I. A. (2005) *Mon. Not. R. Astron. Soc., 356,* 1201.
Bate M. R. et al. (2003) *Mon. Not. R. Astron. Soc., 339,* 577.
Bertoldi F. (1989) *Astrophys. J., 346,* 735.
Bertoldi F. and McKee C. F. (1990) *Astrophys. J., 354,* 529.
Beuther H. et al. (2002) *Astron. Astrophys., 383,* 892.
Beuther H. et al. (2003) *Astron. Astrophys., 408,* 601.
Billot N. et al. (2010) *Astrophys. J., 712,* 797.
Binney J. and Tremaine S. (1987) In *Galactic Dynamics* (J. Ostriker, ed.), Princeton Univ., Princeton. 755 pp.

Bisbas T. G. et al. (2011) *Astrophys. J., 736,* 142.
Bonnell I. A. et al. (1997) *Mon. Not. R. Astron. Soc., 285,* 201.
Bonnell I. A. et al. (2003) *Mon. Not. R. Astron. Soc., 343,* 413.
Bonnell I. A. et al. (2004) *Mon. Not. R. Astron. Soc., 349,* 735.
Bonnell I. A. et al. (2006) *Mon. Not. R. Astron. Soc., 368,* 1296.
Bontemps S. et al. (2010) *Astron. Astrophys., 524,* A18.
Boss A. P. (1983) *Icarus, 55,* 181.
Boss A. P. (1984) *Astrophys. J., 277,* 768.
Boss A. P. (1986) *Astrophys. J. Suppl., 62,* 519.
Boss A. P. et al. (2000) *Astrophys. J., 528,* 325.
Bournaud F. et al. (2014) *Astrophys. J., 780,* 57.
Bruderer S. et al. (2010) *Astrophys. J., 720,* 1432.
Capriotti E. R. and Kozminski J. F. (2001) *Publ. Astron. Soc. Pac., 113,* 677.
Carroll J. J. et al. (2009) *Astrophys. J., 695,* 1376.
Castor J. et al. (1975a) *Astrophys. J. Lett., 200,* L107.
Castor J. I. et al. (1975b) *Astrophys. J., 195,* 157.
Cerviño M. and Luridiana V. (2004) *Astron. Astrophys., 413,* 145.
Chabrier G. (2005) In *The Initial Mass Function 50 Years Later* (E. Corbelli et al., eds.), p. 41. Astrophys. Space Sci. Library, Vol. 327, Kluwer, Dordrecht.
Chakrabarti S. and McKee C. F. (2005) *Astrophys. J., 631,* 792.
Chauhan N. et al. (2009) *Mon. Not. R. Astron. Soc., 396,* 964.
Chevalier R. A. and Clegg A. W. (1985) *Nature, 317,* 44.
Chu Y.-H. and Kennicutt R. C. Jr. (1994) *Astrophys. J., 425,* 720.
Clark P. C. et al. (2005) *Mon. Not. R. Astron. Soc., 359,* 809.
Clarke C. J. et al. (2001) *Mon. Not. R. Astron. Soc., 328,* 485.
Commerçon B. et al. (2010) *Astron. Astrophys., 510,* L3.
Commerçon B. et al. (2011a) *Astrophys. J. Lett., 742,* L9.
Commerçon B. et al. (2011b) *Astron. Astrophys., 530,* A13.
Crutcher R. M. (2012) *Annu. Rev. Astron. Astrophys., 50,* 29.
Cunningham A. J. et al. (2009) *Astrophys. J., 692,* 816.
Cunningham A. J. et al. (2011) *Astrophys. J., 740,* 107.
Curtis E. I. et al. (2010) *Mon. Not. R. Astron. Soc., 408,* 1516.
Dale J. E. and Bonnell I. (2011) *Mon. Not. R. Astron. Soc., 414,* 321.
Dale J. E. and Bonnell I. A. (2008) *Mon. Not. R. Astron. Soc., 391,* 2.
Dale J. E. and Bonnell I. A. (2012) *Mon. Not. R. Astron. Soc., 422,* 1352.
Dale J. E. et al. (2005) *Mon. Not. R. Astron. Soc., 358,* 291.
Dale J. E. et al. (2007) *Mon. Not. R. Astron. Soc., 377,* 535.
Dale J. E. et al. (2011) *Mon. Not. R. Astron. Soc., 411,* 2230.
Dale J. E. et al. (2012a) *Mon. Not. R. Astron. Soc., 427,* 2852.
Dale J. E. et al. (2012b) *Mon. Not. R. Astron. Soc., 424,* 377.
Dale J. E. et al. (2013a) *Mon. Not. R. Astron. Soc., 431,* 1062.
Dale J. E. et al. (2013b) *Mon. Not. R. Astron. Soc., 430,* 234.
da Silva R. L. et al. (2012) *Astrophys. J., 745,* 145.
Davies B. et al. (2011) *Mon. Not. R. Astron. Soc., 416,* 972.
Davis S. W. et al. (2012) *Astrophys. J. Suppl., 199,* 9.
Deharveng L. et al. (2008) *Astron. Astrophys., 482,* 585.
Deharveng L. et al. (2010) *Astron. Astrophys., 523,* A6.
Dent W. R. F. et al. (2009) *Mon. Not. R. Astron. Soc., 395,* 1805.
Dickey J. M. et al. (2013) *Publ. Astron. Soc. Australia, 30,* e003.
Duarte-Cabral A. et al. (2012) *Astron. Astrophys., 543,* A140.
Ekström S. et al. (2012) *Astron. Astrophys., 537,* A146.
Evans N. J. et al. (2009) *Astrophys. J. Suppl., 181,* 321.
Fall S. M. and Chandar R. (2012) *Astrophys. J., 752,* 96.
Fall S. M. et al. (2010) *Astrophys. J. Lett., 710,* L142.
Federrath C. (2013) *Mon. Not. R. Astron. Soc., 436,* 3167.
Federrath C. and Klessen R. S. (2012) *Astrophys. J., 761,* 156.
Feigelson E. et al. (2007) In *Protostars and Planets V* (B. Reipurth et al., eds.), pp. 313–328. Univ. of Arizona, Tucson.
Franco J. et al. (1990) *Astrophys. J., 349,* 126.
Franco J. et al. (1994) *Astrophys. J., 436,* 795.
Freyer T. et al. (2003) *Astrophys. J., 594,* 888.
Freyer T. et al. (2006) *Astrophys. J., 638,* 262.
Galván-Madrid R. et al. (2008) *Astrophys. J. Lett., 674,* L33.
Galván-Madrid R. et al. (2011) *Mon. Not. R. Astron. Soc., 416,* 1033.
Garcia-Segura G. et al. (1996a) *Astron. Astrophys., 305,* 229.
Garcia-Segura G. et al. (1996b) *Astron. Astrophys., 316,* 133.
Gendelev L. and Krumholz M. R. (2012) *Astrophys. J., 745,* 158.
Genel S. et al. (2012) *Astrophys. J., 745,* 11.
Getman K. V. (2009) *Astrophys. J., 699,* 1454.
Getman K. V. et al. (2012) *Mon. Not. R. Astron. Soc., 426,* 2917.
Gibb A. G. et al. (2004) *Astrophys. J., 616,* 301.
Ginsburg A. et al. (2011) *Mon. Not. R. Astron. Soc., 418,* 2121.

Girichidis P. et al. (2011) *Mon. Not. R. Astron. Soc., 413,* 2741.
Girichidis P. et al. (2012a) *Mon. Not. R. Astron. Soc., 420,* 613.
Girichidis P. et al. (2012b) *Mon. Not. R. Astron. Soc., 420,* 3264.
Goldbaum N. J. et al. (2011) *Astrophys. J., 738,* 101.
Graves S. F. et al. (2010) *Mon. Not. R. Astron. Soc., 409,* 1412.
Gritschneder M. et al. (2009) *Astrophys. J. Lett., 694,* L26.
Gritschneder M. et al. (2010) *Astrophys. J., 723,* 971.
Gutermuth R. A. et al. (2009) *Astrophys. J. Suppl., 184,* 18.
Gutermuth R. A. et al. (2011) *Astrophys. J., 739,* 84.
Hansen C. E. et al. (2012) *Astrophys. J., 747,* 22.
Harper-Clark E. and Murray N. (2009) *Astrophys. J., 693,* 1696.
Hartmann L. et al. (1997) *Astrophys. J., 475,* 770.
Hatchell J. et al. (2013) *Mon. Not. R. Astron. Soc., 429,* L10.
Heiderman A. et al. (2010) *Astrophys. J., 723,* 1019.
Hennebelle P. et al. (2011) *Astron. Astrophys., 528,* A72.
Hollenbach D. et al. (1994) *Astrophys. J., 428,* 654.
Holmberg J. and Flynn C. (2000) *Mon. Not. R. Astron. Soc., 313,* 209.
Hopkins P. F. (2013) *Mon. Not. R. Astron. Soc., 428,* 2840.
Hopkins P. F. et al. (2011) *Mon. Not. R. Astron. Soc., 417,* 950.
Hopkins P. F. et al. (2012a) *Mon. Not. R. Astron. Soc., 421,* 3522.
Hopkins P. F. et al. (2012b) *Mon. Not. R. Astron. Soc., 421,* 3488.
Hosokawa T. and Omukai K. (2009) *Astrophys. J., 691,* 823.
Hosokawa T. et al. (2010) *Astrophys. J., 721,* 478.
Hosokawa T. et al. (2011) *Astrophys. J., 738,* 140.
Hosokawa T. et al. (2012) *Astrophys. J. Lett., 760,* L37.
Jacquet E. and Krumholz M. R. (2011) *Astrophys. J., 730,* 116.
Jappsen A.-K. et al. (2005) *Astron. Astrophys., 435,* 611.
Jiang Y.-F. et al. (2012) *Astrophys. J. Suppl., 199,* 14.
Jiang Y.-F. et al. (2013) *Astrophys. J., 763,* 102.
Juneau S. et al. (2009) *Astrophys. J., 707,* 1217.
Kahn F. D. (1974) *Astron. Astrophys., 37,* 149.
Kendrew S. et al. (2012) *Astrophys. J., 755,* 71.
Kennicutt R. C. and Evans N. J. (2012) *Annu. Rev. Astron. Astrophys., 50,* 531.
Kessel-Deynet O. and Burkert A. (2003) *Mon. Not. R. Astron. Soc., 338,* 545.
Keto E. (2003) *Astrophys. J., 599,* 1196.
Keto E. and Wood K. (2006) *Astrophys. J., 637,* 850.
Kim J.-h. et al. (2013a) *Astrophys. J., 775,* 109.
Kim J.-h. et al. (2013b) *Astrophys. J., 779,* 8.
Kim K.-T. and Koo B.-C. (2001) *Astrophys. J., 549,* 979.
Kim K.-T. and Koo B.-C. (2003) *Astrophys. J., 596,* 362.
Klaassen P. D. and Wilson C. D. (2007) *Astrophys. J., 663,* 1092.
Klassen M. et al. (2012) *Astrophys. J., 758,* 137.
Klein R. I. et al. (1983) *Astrophys. J. Lett., 271,* L69.
Klessen R. S. and Burkert A. (2000) *Astrophys. J. Suppl., 128,* 287.
Klessen R. S. and Burkert A. (2001) *Astrophys. J., 549,* 386.
Klessen R. S. et al. (1998) *Astrophys. J., 501,* L205.
Knee L. B. G. and Sandell G. (2000) *Astron. Astrophys., 361,* 671.
Kratter K. M. and Matzner C. D. (2006) *Mon. Not. R. Astron. Soc., 373,* 1563.
Kratter K. M. et al. (2008) *Astrophys. J., 681,* 375.
Kratter K. M. et al. (2010) *Astrophys. J., 708,* 1585.
Krumholz M. R. (2006) *Astrophys. J. Lett., 641,* L45.
Krumholz M. R. (2011) *Astrophys. J., 743,* 110.
Krumholz M. R. and Dekel A. (2010) *Mon. Not. R. Astron. Soc., 406,* 112.
Krumholz M. R. and Matzner C. D. (2009) *Astrophys. J., 703,* 1352.
Krumholz M. R. and McKee C. F. (2008) *Nature, 451,* 1082.
Krumholz M. R. and Tan J. C. (2007) *Astrophys. J., 654,* 304.
Krumholz M. R. and Thompson T. A. (2012) *Astrophys. J., 760,* 155.
Krumholz M. R. and Thompson T. A. (2013) *Mon. Not. R. Astron. Soc., 434,* 2329.
Krumholz M. R. et al. (2005a) *Astrophys. J. Lett., 618,* L33.
Krumholz M. R. et al. (2005b) In *Massive Star Birth: A Crossroads of Astrophysics* (R. Cesaroni et al., eds.), pp. 231–236. IAU Symp. 227, Cambridge Univ., Cambridge.
Krumholz M. R. et al. (2006) *Astrophys. J., 653,* 361.
Krumholz M. R. et al. (2007a) *Astrophys. J., 671,* 518.
Krumholz M. R. et al. (2007b) *Astrophys. J., 656,* 959.
Krumholz M. R. et al. (2009) *Science, 323,* 754.
Krumholz M. R. et al. (2010) *Astrophys. J., 713,* 1120.
Krumholz M. R. et al. (2011) *Astrophys. J., 740,* 74.
Krumholz M. R. et al. (2012a) *Astrophys. J., 745,* 69.
Krumholz M. R. et al. (2012b) *Astrophys. J., 754,* 71.

Kudritzki R. P. et al. (1999) *Astron. Astrophys., 350,* 970.
Kuiper R. et al. (2011) *Astrophys. J., 732,* 20.
Kuiper R. et al. (2012) *Astron. Astrophys., 537,* A122.
Kurtz S. et al. (1994) *Astrophys. J. Suppl., 91,* 659.
Kurtz S. E. et al. (1999) *Astrophys. J., 514,* 232.
Lada C. J. and Lada E. A. (2003) *Annu. Rev. Astron. Astrophys., 41,* 57.
Larson R. B. (1969) *Mon. Not. R. Astron. Soc., 145,* 271.
Larson R. B. (1985) *Mon. Not. R. Astron. Soc., 214,* 379.
Larson R. B. (2005) *Mon. Not. R. Astron. Soc., 359,* 211.
Leitherer C. et al. (1992) *Astrophys. J., 401,* 596.
Leitherer C. et al. (1999) *Astrophys. J. Suppl., 123,* 3.
Leurini S. et al. (2009) *Astron. Astrophys., 507,* 1443.
Li Z.-Y. and Nakamura F. (2006) *Astrophys. J. Lett., 640,* L187.
Longmore S. N. et al. (2011) *Astrophys. J., 726,* 97.
Lopez L. A. et al. (2011) *Astrophys. J., 731,* 91.
Lopez L. A. et al. (2013) *Astrophys. J.,* submitted, arXiv:1309.5421.
López-Sepulcre A. et al. (2009) *Astron. Astrophys., 499,* 811.
Low C. and Lynden-Bell D. (1976) *Mon. Not. R. Astron. Soc., 176,* 367.
Lu J. R. et al. (2013) *Astrophys. J., 764,* 155.
Mackey J. and Lim A. J. (2011) *Mon. Not. R. Astron. Soc., 412,* 2079.
Mac Low M.-M. et al. (2007) *Astrophys. J., 668,* 980.
Maeder A. and Meynet G. (2000) *Astron. Astrophys., 361,* 159.
Maeder A. and Meynet G. (2010) *New Astron. Rev., 54,* 32.
Masunaga H. and Inutsuka S.-I. (1999) *Astrophys. J., 510,* 822.
Masunaga H. and Inutsuka S.-I. (2000) *Astrophys. J., 531,* 350.
Matzner C. D. (2002) *Astrophys. J., 566,* 302.
Matzner C. D. (2007) *Astrophys. J., 659,* 1394.
Matzner C. D. and McKee C. F. (2000) *Astrophys. J., 545,* 364.
Maury A. J. et al. (2009) *Astron. Astrophys., 499,* 175.
McKee C. F. (1989) *Astrophys. J., 345,* 782.
McKee C. F. et al. (1984) *Astrophys. J. Lett., 278,* L115.
Megeath S. T. et al. (2012) *Astron. J., 144,* 192.
Mellema G. et al. (2006) *Astrophys. J., 647,* 397.
Miao J. et al. (2006) *Mon. Not. R. Astron. Soc., 369,* 143.
Mottram J. C. et al. (2011) *Astrophys. J. Lett., 730,* L33.
Muno M. P. et al. (2006a) *Astrophys. J. Lett., 636,* L41.
Muno M. P. et al. (2006b) *Astrophys. J., 650,* 203.
Murray N. and Rahman M. (2010) *Astrophys. J., 709,* 424.
Murray N. et al. (2010) *Astrophys. J., 709,* 191.
Murray N. et al. (2011) *Astrophys. J., 735,* 66.
Myers A. T. et al. (2011) *Astrophys. J., 735,* 49.
Myers A. T. et al. (2013) *Astrophys. J., 766,* 97.
Nakamura F. and Li Z.-Y. (2007) *Astrophys. J., 662,* 395.
Nakamura F. and Li Z.-Y. (2011) *Astrophys. J., 740,* 36.
Nakamura F. et al. (2011a) *Astrophys. J., 737,* 56.
Nakamura F. et al. (2011b) *Astrophys. J., 726,* 46.
Narayanan G. et al. (2012) *Mon. Not. R. Astron. Soc., 425,* 2641.
Norman C. and Silk J. (1980) *Astrophys. J., 238,* 158.
Offner S. S. R. et al. (2008) *Astrophys. J., 686,* 1174.
Offner S. S. R. et al. (2009) *Astrophys. J., 703,* 131.
Osterbrock D. E. and Ferland G. J. (2006) In *Astrophysics of Gaseous Nebulae and Active Galactic Nuclei* (J. Murdzek, ed.), University Science Books, Mill Valley, California. 461 pp.
Padoan P. and Nordlund Å. (2011) *Astrophys. J., 730,* 40.
Palau A. et al. (2013) *Astrophys. J., 762,* 120.
Palla F. and Stahler S. W. (1991) *Astrophys. J., 375,* 288.
Palla F. and Stahler S. W. (1992) *Astrophys. J., 392,* 667.
Parker J. W. (1993) *Astron. J., 106,* 560.
Patel N. A. et al. (1998) *Astrophys. J., 507,* 241.
Pellegrini E. W. et al. (2011) *Astrophys. J., 738,* 34.
Peters T. et al. (2010a) *Astrophys. J., 711,* 1017.
Peters T. et al. (2010b) *Astrophys. J., 719,* 831.
Peters T. et al. (2011) *Astrophys. J., 729,* 72.
Plunkett A. L. et al. (2013) *Astrophys. J., 774,* 22.
Portegies Zwart S. F. et al. (2010) *Annu. Rev. Astron. Astrophys., 48,* 431.
Price D. J. (2008) *J. Comp. Phys., 227,* 10040.
Price D. J. and Bate M. R. (2008) *Mon. Not. R. Astron. Soc., 385,* 1820.
Price D. J. and Bate M. R. (2009) *Mon. Not. R. Astron. Soc., 398,* 33.
Rathborne J. M. et al. (2008) *Astrophys. J., 689,* 1141.
Read J. I. and Hayfield T. (2012) *Mon. Not. R. Astron. Soc., 422,* 3037.
Rees M. J. (1976) *Mon. Not. R. Astron. Soc., 176,* 483.
Richling S. and Yorke H. W. (1997) *Astron. Astrophys., 327,* 317.
Robitaille T. P. et al. (2006) *Astrophys. J. Suppl., 167,* 256.

Robitaille T. P. et al. (2007) *Astrophys. J. Suppl., 169,* 328.
Rogers H. and Pittard J. M. (2013) *Mon. Not. R. Astron. Soc., 431,* 1337.
Sánchez-Monge Á. et al. (2013) *Astron. Astrophys., 557,* A94.
Sandford M. T. II et al. (1982) *Astrophys. J., 260,* 183.
Sandford M. T. II et al. (1984) *Astrophys. J., 282,* 178.
Schönke J. and TscharnuterW. M. (2011) *Astron. Astrophys., 526,* A139.
Scoville N. Z. et al. (2001) *Astron. J., 122,* 3017.
Shore S. N. (1981) *Astrophys. J., 249,* 93.
Shore S. N. (1983) *Astrophys. J., 265,* 202.
Shu F. H. et al. (1999) In *The Origin of Stars and Planetary Systems* (C. J. Lada and N. D. Kylafis, eds.), p. 193. NATO ASIC Proc. 540, Crete, Greece.
Sicilia-Aguilar A. et al. (2013) *Astron. Astrophys., 551,* A34.
Silich S. and Tenorio-Tagle G. (2013) *Astrophys. J., 765,* 43.
Silva-Villa E. and Larsen S. S. (2011) *Astron. Astrophys., 529,* A25.
Smith N. et al. (2000) *Astrophys. J. Lett., 532,* L145.
Smith N. et al. (2005) *Astron. J., 129,* 888.
Smith N. et al. (2010) *Mon. Not. R. Astron. Soc., 406,* 952.
Snider K. D. et al. (2009) *Astrophys. J., 700,* 506.
Socrates A. and Sironi L. (2013) *Astrophys. J. Lett., 772,* L21.
Spaans M. et al. (1995) *Astrophys. J. Lett., 455,* L167.
Spitzer L. (1978) In *Physical Processes in the Interstellar Medium* (M. F. Bode and A. Evans, eds.), Wiley-VCH, New York. 335 pp.
Stamatellos D. et al. (2011) *Astrophys. J., 730,* 32.
Stamatellos D. et al. (2012) *Mon. Not. R. Astron. Soc., 427,* 1182.
Stanke T. and Williams J. P. (2007) *Astron. J., 133,* 1307.
Stinson G. S. et al. (2013) *Mon. Not. R. Astron. Soc., 428,* 129.
Sugitani K. et al. (1995) *Astrophys. J. Lett., 455,* L39.
Sun K. et al. (2006) *Astron. Astrophys., 451,* 539.
Swift J. J. (2009) *Astrophys. J., 705,* 1456.
Swift J. J. and Welch W. J. (2008) *Astrophys. J. Suppl., 174,* 202.
Tan J. C. et al. (2006) *Astrophys. J. Lett., 641,* L121.
Tenorio-Tagle G. et al. (2007) *Astrophys. J., 658,* 1196.
Thompson M. A. et al. (2012) *Mon. Not. R. Astron. Soc., 421,* 408.
Thompson T. A. et al. (2005) *Astrophys. J., 630,* 167.
Toalá J. A. and Arthur S. J. (2011) *Astrophys. J., 737,* 100.
Tomida K. et al. (2010a) *Astrophys. J. Lett., 725,* L239.
Tomida K. et al. (2010b) *Astrophys. J. Lett., 714,* L58.
Tout C. A. et al. (1999) *Mon. Not. R. Astron. Soc., 310,* 360.
Townsley L. K. et al. (2003) *Astrophys. J., 593,* 874.
Townsley L. K. et al. (2006) *Astron. J., 131,* 2140.
Townsley L. K. et al. (2011) *Astrophys. J. Suppl., 194,* 15.
Tremblin P. et al. (2012a) *Astron. Astrophys., 538,* A31.
Tremblin P. et al. (2012b) *Astron. Astrophys., 546,* A33.
Urban A. et al. (2009) *Astrophys. J., 698,* 1341.
Urban A. et al. (2010) *Astrophys. J., 710,* 1343.
Urquhart J. S. et al. (2007) *Astron. Astrophys., 467,* 1125.
van Kempen T. A. et al. (2009a) *Astron. Astrophys., 501,* 633.
van Kempen T. A. et al. (2009b) *Astron. Astrophys., 507,* 1425.
van Kempen T. A. et al. (2010) *Astron. Astrophys., 518,* L121.
Varricatt W. P. et al. (2010) *Mon. Not. R. Astron. Soc., 404,* 661.
Vázquez G. A. and Leitherer C. (2005) *Astrophys. J., 621,* 695.
Vázquez-Semadeni E. et al. (2010) *Astrophys. J., 715,* 1302.
Verdolini S. et al. (2013) *Astrophys. J., 769,* 12.
Vink J. S. et al. (2000) *Astron. Astrophys., 362,* 295.
Vink J. S. et al. (2001) *Astron. Astrophys., 369,* 574.
Visser R. et al. (2012) *Astron. Astrophys., 537,* A55.
Walawender J. et al. (2005) *Astron. J., 129,* 2308.
Walawender J. et al. (2008) In *Handbook of Star Forming Regions, Volume I* (B. Reipurth, ed.), p. 346. ASP Monograph, Astronomical Society of the Pacific, San Francisco.
Walch S. et al. (2013) *Mon. Not. R. Astron. Soc., 435,* 917.
Walch S. K. et al. (2012) *Mon. Not. R. Astron. Soc., 427,* 625.
Walmsley M. (1995) *Rev. Mex. Astron. Astrofis. Ser. Conf., 1,* 137.
Wang K. et al. (2011) *Astrophys. J., 735,* 64.
Wang K. et al. (2012a) *Astrophys. J. Lett., 745,* L30.
Wang K. et al. (2012b) *Astrophys. J. Lett., 745,* L30.
Wang P. et al. (2010) *Astrophys. J., 709,* 27.
Wang Y. et al. (2008) *Astrophys. J. Lett., 672,* L33.
Watson C. et al. (2008) *Astrophys. J., 681,* 1341.
Weaver R. et al. (1977) *Astrophys. J., 218,* 377.
Whitehouse S. C. and Bate M. R. (2006) *Mon. Not. R. Astron. Soc., 367,* 32.
Whitworth A. (1979) *Mon. Not. R. Astron. Soc., 186,* 59.

Whitworth A. P. et al. (1994a) *Astron. Astrophys., 290,* 421.
Whitworth A. P. et al. (1994b) *Mon. Not. R. Astron. Soc., 268,* 291.
Williams J. P. et al. (2003) *Astrophys. J., 591,* 1025.
Williams R. J. R. et al. (2001) *Mon. Not. R. Astron. Soc., 327,* 788.
Wise J. H. et al. (2012) *Mon. Not. R. Astron. Soc., 427,* 311.
Wolfire M. G. and Cassinelli J. P. (1986) *Astrophys. J., 310,* 207.
Wolfire M. G. and Cassinelli J. P. (1987) *Astrophys. J., 319,* 850.
Wood D. O. S. and Churchwell E. (1989) *Astrophys. J. Suppl.,*
    69, 831.
Wu Y. et al. (2005) *Astron. J., 129,* 330.
Wünsch R. et al. (2010) *Mon. Not. R. Astron. Soc., 407,* 1963.

Xie T. and Goldsmith P. F. (1994) *Astrophys. J., 430,* 252.
Yeh S. C. C. and Matzner C. D. (2012) *Astrophys. J., 757,* 108.
Yeh S. C. C. et al. (2013) *Astrophys. J., 769,* 11.
Yildiz U. A. et al. (2012) *Astron. Astrophys., 542,* A86.
Yorke H. W. and Kruegel E. (1977) *Astron. Astrophys., 54,* 183.
Yorke H. W. and Sonnhalter C. (2002) *Astrophys. J., 569,* 846.
Yorke H. W. and Welz A. (1996) *Astron. Astrophys., 315,* 555.
Zhang Q. and Wang K. (2011) *Astrophys. J., 733,* 26.
Zhang Q. et al. (2005) *Astrophys. J., 625,* 864.
Zhang Q. et al. (2009) *Astrophys. J., 696,* 268.
Zuckerman B. and Evans N. J. (1974) *Astrophys. J. Lett., 192,* L149.